

MichiganTech
Transportation Institute

**Impact of Hydrated Cement Paste Quality
and Entrained Air-Void System on the
Durability of Concrete: Final Report**

Michigan Department of Transportation
Report No. RC-1552

*“Meeting our transportation needs through
innovative research, distinctive educational
programs, technology transfer, and workforce
development.”*

Karl W. Peterson, Ph.D.
Michigan Technological University
1400 Townsend Drive
Houghton, MI 49931
krpeters@mtu.edu

Lawrence L. Sutter, Ph.D.
Michigan Technological University
1400 Townsend Drive
Houghton, MI 49931
llsutter@mtu.edu

MichiganTech
1400 Townsend Drive
Houghton, MI 49931

June 30, 2011

Technical Report Documentation Page

1. Report No. RC-1552	2. Government Accession No.	3. MDOT Project Manager J. Staton	
4. Title and Subtitle Impact of Hydrated Cement Paste Quality and Entrained Air-Void System on the Durability of Concrete		5. Report Date June 30, 2011	
		6. Performing Organization Code	
7. Author(s) Karl Peterson, Lawrence Sutter		8. Performing Org. Report No.	
9. Performing Organization Name and Address Michigan Tech Transportation Institute 1400 Townsend Dr Houghton Michigan 49931		10. Work Unit No. (TRAIS)	
		11. Contract No. 2006-0414	
		11(a). Authorization No. 10	
12. Sponsoring Agency Name and Address Michigan Department of Transportation PO Box 30049 Lansing, Michigan 48909		13. Type of Report & Period Covered Final	
		14. Sponsoring Agency Code	
15. Supplementary Notes			
16. Abstract <p>This study is designed to examine whether traditional limits used to describe the air-void system still apply to concrete prepared with new admixtures and materials. For this research, the concrete mixtures prepared were characterized with traditional and emerging equipment and tests used to measure hydrated cement paste properties. All concrete mixtures were prepared using materials that meet current MDOT specifications.</p> <p>Modern cements and the use of supplementary cementitious materials lead to a hardened cement paste that can potentially have a higher tensile strength and lower permeability. The classic limitation of an air-void system spacing factor less than or equal to 0.2 mm is still a safe value to ensure F-T durability, but evidence exists that concrete mixtures with a spacing factor greater than 0.2 mm can also be F-T durable. The durability of concretes produced with a reduced cementitious material content (CMC), in terms of the laboratory ASTM C666 testing conducted in this study, is superior to traditional 564 lbs/yd³ CMC concrete.</p> <p>There is general agreement between methods of measuring the total air content of a concrete mixture, although the AVA generally does not perform well for this task. Test results for water content by AASHTO T 318 compared well with the mixture designs when the measured water content is corrected for aggregate absorption. Test results for <i>w/cm</i> by the Cementometer™ were not as promising, but may be improved with further attention to the calibration process. Semi-adiabatic calorimetry proved to be useful tool for identifying delayed-set mixtures.</p>			
17. Key Words freeze-thaw, cement paste, air void, fly ash, slag cement, SCM, air void analyzer, AVA, AASHTO T 318, Cementometer		18. Distribution Statement No restrictions. This document is available to the public through the Michigan Department of Transportation.	
19. Security Classification - report	20. Security Classification - page	21. No. of Pages 120 + 1 Appendix (9 pages)	22. Price

Disclaimer

The contents of this report reflect the views of the authors, who are responsible for the facts and accuracy of the information presented herein. The contents do not necessarily reflect the views of the Michigan Department of Transportation or the Federal Highway Administration. This report does not constitute a standard, specification, or regulation.

Acknowledgements

The authors acknowledge support provided by the staff of the University Transportation Center (UTC) for Materials in Sustainable Transportation Infrastructure at Michigan Technological University in conducting this research. The UTC Program is administered by the U.S. Department of Transportation's Research and Innovative Technology Administration (RITA). The views presented in this report are those of the authors and not necessarily the views of RITA or the U.S. Department of Transportation.

The authors also acknowledge the contribution of Michigan Tech Research Engineers Michael Yokie and Matthew King, Graduate Research Assistant Jacob Vermillion, and undergraduate students Benjamin Longmire and Nicholas Weinmann in completing this research.

Table of Contents

List of Figures	iii
List of Tables	ix
Executive Summary	1
1. Introduction.....	3
2. Objective.....	4
3. Scope.....	4
4. Methodology.....	4
4.1 Mixture Design Experimental Matrices.....	4
4.1.1 Phase II Mixtures	4
4.1.2 Phase III Mixtures.....	6
4.2 Materials	6
4.2.1 Physical Properties of Materials	6
4.2.2 Aggregate Gradations	8
5. Test Results.....	13
5.1 Fresh Concrete Tests.....	13
5.1.1 Standard Fresh Concrete Tests.....	13
5.1.2 Additional Fresh Concrete Tests.....	13
5.1.3 Calorimetry Curves from Exploration of Delayed Set Mixture.....	27
5.2 Hardened Concrete Tests	29
5.2.1 Absorptivity, F-T, Compressive Strength, and Maturity	29
5.2.2 Additional F-T Testing	29
5.2.3 Air-Void System Parameters	58
5.2.4 Petrographic Examination for Determination of Equivalent w/cm	60
5.2.5 Petrographic Examination of Selected Mixtures.	70
5.2.6 Characterization of Cement for CEMHYD3D Modeling of Capillary Pore Structure 76	
5.2.6.1 Particle Size Distribution	76
5.2.6.2 Partitioning of Cement Clinker Particles into Cement Phases.....	80
5.2.6.3 Cement Alkalis.....	80
5.2.6.4 Determination of Cycle to Time Conversion Factor.....	83
5.2.7 Execution of the Hydration Model	85
5.2.8 Scanning Electron Microscope Examination of Thin Sections	87

6. Discussion of Results	90
6.1 Fresh Concrete Test Results.....	90
6.1.1 Temperature: Fresh Concrete and Semi-Adiabatic Calorimetry	90
6.1.2 Slump	90
6.1.3 Air Content.....	91
6.1.4 Water Content and w/cm Testing	91
6.2 Hardened Concrete Test Results.....	94
6.2.1 Compressive Strength and Maturity	94
6.2.2 Absorptivity	95
6.2.3 Epifluorescent Determination of Equivalent w/cm.....	95
6.2.4 F-T Testing.....	97
6.3 F-T Performance Related to Other Parameters	98
6.3.1 Air-void Parameters and F-T Performance.....	98
6.3.2 SCM Replacement and F-T Performance	107
6.3.3 Absorptivity and F-T Performance	110
6.3.4 AEA Type and F-T Performance.....	111
6.3.5 Duplicate Concrete Mixtures that Exhibited Variable F-T Performance	113
6.3.6 Insights from CEMHYD3D Modeling to F-T Performance.....	113
6.4 Mixtures Exhibiting Delayed Set.....	114
7. Conclusions.....	115
8. Recommendations for Implementation & Further Research	117
9. List of Acronyms, Abbreviations and Symbols.....	118
10. References.....	119
11. Appendix - Input for execution of CEMHYD3D v3.0 models.....	A1

List of Figures

Figure 1: MDOT 2NS gradation limits and as-received fine aggregate gradations from Superior S&G pit and Lindberg Co. Rd. 480 pit.	9
Figure 2: MDOT 6A/6AA gradation limits and as-received coarse aggregate gradations from Presque Isle limestone quarry.	9
Figure 3: MDOT 6AAA gradation limits and manufactured optimized coarse aggregate gradations from Presque Isle limestone.	10
Figure 4: Percent retained “haystack” chart with recommended MDOT optimized gradation limits, and combined aggregate gradations for the gap-graded concrete mixtures.	11
Figure 5: Shilstone coarseness factor - workability factor chart with recommended MDOT optimized gradation limits, and locations of the gap-graded concrete mixtures.	11
Figure 6: Percent retained “haystack” chart with recommended MDOT optimized gradation limits, and combined aggregate gradations for the optimized concrete mixtures.	12
Figure 7: Shilstone coarseness factor - workability factor chart with recommended MDOT optimized gradation limits, and locations of the optimized concrete mixtures.	12
Figure 8: Slump of fresh concrete for Phase II 0.45 w/cm 564 lbs/yd ³ CMC mixtures. From top to bottom, high air content and low air content mixtures.	17
Figure 9: Slump of fresh concrete for Phase II 0.45 w/cm 470 lbs/yd ³ CMC mixtures. From top to bottom, high air content and low air content mixtures.	18
Figure 10: Slump of fresh concrete for Phase II 0.50 w/cm 564 lbs/yd ³ CMC mixtures. From top to bottom, high air content and low air content mixtures.	19
Figure 11: Slump of fresh concrete for Phase II 0.52 w/cm 517 lbs/yd ³ CMC mixtures. From top to bottom, high air content and low air content mixtures.	20
Figure 12: Slump of fresh concrete for Phase III 0.46 w/cm very low air content mixtures. From top to bottom, 564 lbs/yd ³ and 490 lbs/yd ³ CMC mixtures.	21
Figure 13: Air content pressure meter test results grouped according to mixture design target air contents.	22
Figure 14: Calorimetry plots for the Phase II 0.45 w/cm 564 lbs/yd ³ CMC mixtures. From left to right, high air content mixtures vs. low air content mixtures.	23
Figure 15: Calorimetry plots for the Phase II 0.45 w/cm 470 lbs/yd ³ CMC mixtures. From left to right, high air content mixtures vs. low air content mixtures.	24
Figure 16: Calorimetry plots for the Phase II 0.50 w/cm 564 lbs/yd ³ CMC mixtures. From left to right, high air content mixtures vs. low air content mixtures.	25
Figure 17: Calorimetry plots for the Phase II 0.52 w/cm 517 lbs/yd ³ CMC mixtures. From left to right, high air content mixtures vs. low air content mixtures.	26

Figure 18: Calorimetry curves for delayed initial and final set mixture and repeat mixtures.	28
Figure 19: Calorimetry curves for delayed set mixture and repeat mixtures with double the water reducer dosage.	28
Figure 20: Compressive strength gain plots for the 0.45 <i>w/cm</i> 564 lbs/yd ³ CMC mixtures. From left to right, high air content mixtures vs. low air content mixtures.	36
Figure 21: Compressive strength gain plots for the 0.45 <i>w/cm</i> 470 lbs/yd ³ CMC mixtures. From left to right, high air content mixtures vs. low air content mixtures.	37
Figure 22: Compressive strength gain plots for the 0.50 <i>w/cm</i> 564 lbs/yd ³ CMC mixtures. From left to right, high air content mixtures vs. low air content mixtures.	38
Figure 23: Compressive strength gain plots for the 0.52 <i>w/cm</i> 517 lbs/yd ³ CMC mixtures. From left to right, high air content mixtures vs. low air content mixtures.	39
Figure 24: Compressive strength gain plots for the Phase III very low air content 0.46 <i>w/cm</i> mixtures. From left to right, 564 lbs/yd ³ CMC mixtures vs. 490 lbs/yd ³ CMC mixtures.	40
Figure 25: Absorptivity plots for the 0.45 <i>w/cm</i> 564 lbs/yd ³ CMC mixtures.	41
Figure 26: Absorptivity plots for the 0.45 <i>w/cm</i> 470 lbs/yd ³ CMC mixtures.	42
Figure 27: Absorptivity plots for the 0.50 <i>w/cm</i> 564 lbs/yd ³ CMC mixtures.	43
Figure 28: Absorptivity plots for the 0.52 <i>w/cm</i> 517 lbs/yd ³ CMC mixtures.	44
Figure 29: Absorptivity plots for the Phase III very low air content 0.46 <i>w/cm</i> mixtures.	45
Figure 30: Relative dynamic modulus of elasticity plots for the 0.45 <i>w/cm</i> 564 lbs/yd ³ CMC mixtures frozen in air (ASTM C666 Procedure B).	46
Figure 31: Relative dynamic modulus of elasticity plots for the 0.45 <i>w/cm</i> 470 lbs/yd ³ CMC mixtures frozen in air (ASTM C666 Procedure B).	47
Figure 32: Relative dynamic modulus of elasticity plots for the 0.50 <i>w/cm</i> 564 lbs/yd ³ CMC mixtures frozen in air (ASTM C666 Procedure B).	48
Figure 33: Relative dynamic modulus of elasticity plots for the 0.52 <i>w/cm</i> 517 lbs/yd ³ CMC mixtures frozen in air (ASTM C666 Procedure B).	49
Figure 34: Relative dynamic modulus of elasticity plots for the Phase III very low air content 0.46 <i>w/cm</i> mixtures frozen in air (ASTM C666 Procedure B).	50
Figure 35: Relative dynamic modulus of elasticity plots for the Phase III very low air content 0.46 <i>w/cm</i> mixtures frozen in water (ASTM C666 Procedure A).	51
Figure 36: Relative dynamic modulus of elasticity plots for the Phase III very low air content 0.46 <i>w/cm</i> mixtures frozen in a 4.0 wt. % CaCl ₂ brine.	52

Figure 37: Weight change plots for the Phase III very low air content 0.46 <i>w/cm</i> mixtures frozen in air (ASTM C666 Procedure B).....	53
Figure 38: Weight change plots for the Phase III very low air content 0.46 <i>w/cm</i> mixtures frozen in water (ASTM C666 Procedure A).....	54
Figure 39: Weight change plots for the Phase III very low air content 0.46 <i>w/cm</i> mixtures frozen in a 4.0 wt. % CaCl ₂ brine.....	55
Figure 40: Relative dynamic modulus of elasticity plots from selected Phase II concrete mixtures exposed to extended F-T cycling test results under different ASTM C66 Procedure A freezing regimes.....	56
Figure 41: Weight change plots from selected Phase II concrete mixtures exposed to extended F-T cycling test results under different ASTM C66 Procedure A freezing regimes.....	57
Figure 42: Average absolute deviation between flatbed scanner and manual ASTM 457 measurements of air content and void frequency versus threshold for the 20 training samples. .	59
Figure 43: Histogram of optimum threshold levels determined for the 20 training samples.	59
Figure 44: Comparison of air-void parameters measured from manual ASTM C457 and flatbed scanner at a threshold of 151.	60
Figure 45: Mosaic of twelve images collected from 0.40 <i>w/cm</i> mortar standard (left), and after masking air-voids and sand to isolate fluorescence from the cement paste (right).	62
Figure 46: Mosaic of twelve images collected from 0.50 <i>w/cm</i> mortar standard (left), and after masking air-voids and sand to isolate fluorescence from the cement paste (right).	63
Figure 47: Mosaic of twelve images collected from 0.60 <i>w/cm</i> mortar standard (left), and after masking air-voids and sand to isolate fluorescence from the cement paste (right).	64
Figure 49: Mosaic of twelve images collected from LO-VR-PC-6SK-45WC mixture (left), and after masking air-voids and sand to isolate fluorescence from the cement paste (right).....	65
Figure 50: Mosaic of twelve images collected from LO-VR-PC-6SK-50WC mixture (left), and after masking air-voids and sand to isolate fluorescence from the cement paste (right).....	66
Figure 51: Mosaic of twelve images collected from LO-VR-PC-5.5SK-52WC mixture (left), and after masking air-voids and sand to isolate fluorescence from the cement paste (right).....	67
Figure 52: Mosaic of twelve images collected from LO-SYN-PC-6SK-45WC mixture (left), and after masking air-voids and sand to isolate fluorescence from the cement paste (right).....	68
Figure 53: Mosaic of twelve images collected from LO-SYN-PC-6SK-50WC mixture (left), and after masking air-voids and sand to isolate fluorescence from the cement paste (right).....	69
Figure 54: Mosaic of twelve images collected from LO-SYN-PC-5.5SK-52WC mixture (left), and after masking air-voids and sand to isolate fluorescence from the cement paste (right).	70

Figure 55: Mosaic of twelve images collected from the good F-T performance LO-VR-SLG-5SK-45WC mixture (left), and after masking air-voids and sand to isolate fluorescence from the cement paste (right).....	71
Figure 56: Mosaic of twelve images collected from the poor F-T performance LO-VR-SLG-5SK-45WC mixture (left), and after masking air-voids and sand to isolate fluorescence from the cement paste (right).....	72
Figure 57: Mosaic of twelve images collected from the good F-T performance LO-SYN-FA-6SK-45WC mixture (left), and after masking air-voids and sand to isolate fluorescence from the cement paste (right).....	73
Figure 58: Mosaic of twelve images collected from the poor F-T performance LO-SYN-FA-6SK-45WC mixture (left), and after masking air-voids and sand to isolate fluorescence from the cement paste (right).....	74
Figure 59: Mosaic of twelve images collected from the normal set LO-VR-SLG-6SK-45WC mixture (left), and after masking air-voids and sand to isolate fluorescence from the cement paste (right).	75
Figure 60: Mosaic of twelve images collected from delayed set LO-SYN-SLG-6SK-45WC mixture (left), and after masking air-voids and sand to isolate fluorescence from the cement paste (right).	76
Figure 61: Clockwise from upper left: BSE image, binary image resulting from the application of a threshold of 85, after filling of holes and removal particles touching the edge, and approximation of particle profiles by ellipses.....	77
Figure 62: Portland cement particle size distributions as measured using different threshold levels.	78
Figure 63: From left to right, depictions of voxelized spheres with diameters of 1, 3, and 5 voxels, and volumes of 1, 19, and 81 voxels respectively.....	78
Figure 63: 2D slices from 3D models to illustrate steps in the CEMHYD3D process.....	79
Figure 64: BSE image and elemental maps collected from polished cross-section through portland cement grains embedded in epoxy resin.....	81
Figure 65: Classified image output (top) and after application of median filter to remove noise (bottom) to show major cement phases.	82
Figure 66: Depiction of chemical shrinkage experimental set-up, after Tazawa et al., [1995]. ..	83
Figure 67: Laboratory and model chemical shrinkage data for 0.45 <i>w/cm</i> cement paste at cycle to time conversion factor of 0.00035.	84
Figure 68: Laboratory and model chemical shrinkage data for 0.50 <i>w/cm</i> cement paste at cycle to time conversion factor of 0.00040.	84

Figure 69: Laboratory and model chemical shrinkage data for 0.52 <i>w/cm</i> cement paste at cycle to time conversion factor of 0.00100.	85
Figure 70: Total porosity versus time from the hydration models.....	86
Figure 71: Fraction of connected porosity across the 0.1 mm width of the cube versus time from the hydration models.....	86
Figure 72: Slice from CEMHYD3D output for 0.45 <i>w/cm</i> system at 120 days (center tile) compared to BSE images from polished thin sections prepared from 120 day moist-cured 0.45 <i>w/cm</i> concrete mixture (surrounding tiles).	87
Figure 73: Slice from CEMHYD3D output for 0.50 <i>w/cm</i> system at 120 days (center tile) compared to BSE images from polished thin sections prepared from 120 day moist-cured 0.50 <i>w/cm</i> concrete mixture (surrounding tiles).	88
Figure 74: Slice from CEMHYD3D output for 0.52 <i>w/cm</i> system at 120 days (center tile) compared to BSE images from polished thin sections prepared from 120 day moist-cured 0.52 <i>w/cm</i> concrete mixture (surrounding tiles).	89
Figure 75: Microwave oven drying test water content results versus mix design.	92
Figure 76: <i>w/cm</i> values as measured by the Cementometer™ using the default factory calibration plotted against mixture design <i>w/cm</i> values.....	93
Figure 77: <i>w/cm</i> values for slag cement mixtures as measured by the Cementometer™ using in-house calibration plotted against mixture design <i>w/cm</i> values.	93
Figure 78: Equivalent <i>w/cm</i> values for vinsol resin AEA portland cement concrete mixtures as measured by paste fluorescence plotted against mixture design <i>w/cm</i> values.....	96
Figure 79: Equivalent <i>w/cm</i> values for synthetic AEA portland cement concrete mixtures as measured by paste fluorescence plotted against mixture design <i>w/cm</i> values.....	96
Figure 80: Equivalent <i>w/cm</i> measurements from concrete mixtures made with <i>w/cm</i> of 0.45, both with and without SCMs.	97
Figure 81: Air content measured by ASTM C173 (volumetric meter) ASTM C138 (gravimetric air) the AVA and flatbed scanner compared to that measured by the pressure meter.....	99
Figure 82: Comparison of specific surface measurements using AVA and flatbed scanner.....	102
Figure 83: Comparison of spacing factor measurements using AVA and flatbed scanner.	102
Figure 84: Measured specific surface versus measured spacing factor by flatbed scanner and the AVA.....	103
Figure 85: Volume fractions of cement paste within 0.2 mm (a), 0.1 mm (b), 0.05 mm (c), and 0.025 mm of an air-void (d) for all concrete mixtures, plotted against spacing factor, and color-coded in terms of the ASTM C666 durability factor.	104

Figure 86: Philleo factor vs. spacing factor for all concrete mixtures, plotted in terms of concrete mixture target air content and ASTM C666 durability factor.....	105
Figure 87: Paste content (total concrete volume minus aggregate and air volumes) vs. pressure meter air content for all concrete mixtures plotted according to durability factor, CMC, and <i>w/cm</i>	105
Figure 88: Chord length size distribution plots color-coded in terms of durability factor for (a) high target air content mixtures, (b) low air content target mixtures, and (c) very low air content target mixtures.	107
Figure 89: Air content measurements for the 564 lbs/yd ³ CMC mixtures made at a <i>w/cm</i> of 0.45 and 0.46, plotted in terms of durability factor and SCM content.	109
Figure 90: Paste content (total concrete volume minus aggregate and air volumes) for the 564 lbs/yd ³ CMC mixtures made at a <i>w/cm</i> of 0.45 and 0.46, plotted in terms of durability factor and SCM content.	109
Figure 91: Absorptivity curves color-coded in terms of durability factor for (a) high target air content mixtures, (b) low air content target mixtures, and (c) very low air content target mixtures.	110
Figure 92: Chord length size distribution plots color-coded in terms of AEA type, (a) high target air content mixtures, (b) low air content target mixtures, and (c) very low air content target mixtures.....	112

List of Tables

Table 1: Phase II mixture design experimental matrix.	5
Table 2: Phase III mixture design experimental matrix.	7
Table 3: Physical properties of materials.	8
Figure 4: Shilstone haystack chart with recommended MDOT optimized gradation limits, and combined aggregate gradations for the gap-graded concrete mixtures.	11
Figure 5: Shilstone coarseness factor - workability factor chart with recommended MDOT optimized gradation limits, and locations of the gap-graded concrete mixtures.	11
Figure 6: Shilstone haystack chart with recommended MDOT optimized gradation limits, and combined aggregate gradations for the optimized concrete mixtures.	12
Figure 7: Shilstone coarseness factor - workability factor chart with recommended MDOT optimized gradation limits, and locations of the optimized concrete mixtures.	12
Table 4: Fresh concrete test results and air-void parameters for Phase II high air-content mixtures.	14
Table 5: Fresh concrete test results and air-void parameters for Phase II low air-content mixtures.	15
Table 6: Fresh concrete test results and air-void parameters for Phase III very low air-content mixtures.	16
Table 7: Hardened concrete test results for absorptivity, F-T durability, and compressive strength for Phase II high air content mixtures.	30
Table 8: Hardened concrete test results for absorptivity, F-T durability, and compressive strength for Phase II low air content mixtures.	31
Table 9: Hardened concrete test results for absorptivity, F-T durability, and compressive strength for Phase III very low air content mixtures.	32
Table 10: F-T test results under different freezing regimes for Phase III very low air content mixtures.	32
Table 11: Maturity test results for Phase II high air content mixtures.	33
Table 12: Maturity test results for Phase II low air content mixtures.	34
Table 13: F-T test results under different freezing regimes for extended F-T cycling on selected Phase II concrete mixtures.	35
Table 14: Average fluorescence values from cement paste for each image collected from 0.40 w/cm mortar standard, and correlated equivalent w/cm values based on calibration curve.	62
Table 15: Average fluorescence values from cement paste for each image collected from 0.50 w/cm mortar standard, and correlated equivalent w/cm values based on calibration curve.	63

Table 16: Average fluorescence values from cement paste for each image collected from 0.60 w/cm mortar standard, and correlated equivalent w/cm values based on calibration curve..... 64

Table 17: Average fluorescence values from cement paste for each image collected from LO-VR-PC-6SK-45WC mixture, and correlated equivalent w/cm values based on calibration curve. 65

Table 18: Average fluorescence values from cement paste for each image collected from LO-VR-PC-6SK-50WC mixture, and correlated equivalent w/cm values based on calibration curve. 66

Table 19: Average fluorescence values from cement paste for each image collected from LO-VR-PC-5.5SK-52WC mixture, and correlated equivalent w/cm values based on calibration curve. 67

Table 20: Average fluorescence values from cement paste for each image collected from LO-SYN-PC-6SK-45WC mixture, and correlated equivalent w/cm values based on calibration curve. 68

Table 21: Average fluorescence values from cement paste for each image collected from LO-SYN-PC-6SK-50WC mixture, and correlated equivalent w/cm values based on calibration curve. 69

Table 22: Average fluorescence values from cement paste for each image collected from LO-SYN-PC-5.5SK-52WC mixture, and correlated equivalent w/cm values based on calibration curve..... 70

Table 23: Average fluorescence values from cement paste for each image collected from the poor F-T performance LO-VR-SLG-5SK-50WC mixture, and correlated equivalent w/cm values based on calibration curve. 71

Table 24: Average fluorescence values from cement paste for each image collected from the poor F-T performance LO-VR-SLG-5SK-50WC mixture, and correlated equivalent w/cm values based on calibration curve. 72

Table 25: Average fluorescence values from cement paste for each image collected from the good F-T performance LO-SYN-FA-6SK-45WC mixture, and correlated equivalent w/cm values based on calibration curve. 73

Table 26: Average fluorescence values from cement paste for each image collected from the poor F-T performance LO-SYN-FA-6SK-45WC mixture, and correlated equivalent w/cm values based on calibration curve. 74

Table 27: Average fluorescence values from cement paste for each image collected from the normal set LO-VR-SLG-6SK-45WC mixture, and correlated equivalent w/cm values based on calibration curve..... 75

Table 28: Average fluorescence values from cement paste for each image collected from the delayed set LO-SYN-SLG-6SK-45WC mixture, and correlated equivalent w/cm values based on calibration curve..... 76

Table 29: Summary of how the low and very low target air mixtures would be classified for F-T durability based upon ASTM C457 results, and also a summary of how many low and very low target air mixtures actually failed ASTM C666 testing with a durability factor less than 85 at 300 cycles..... 108

Table 30: Summary statistics for air-void parameters as measured by flatbed scanner. 112

Executive Summary

In cold climates, concrete used in pavements and bridges must be able to withstand cyclic freezing and thawing (F-T). This study is designed to examine whether traditional limits used to describe the air-void system still apply to concrete prepared with these new admixtures and materials. Overall this research examines the relationship(s) between F-T durability and the quality of hydrated cement paste (HCP) integral to the concrete. The HCP system is generally thought of as hydration products from the chemical reaction of portland cement, supplementary cementitious materials (SCMs), and water, but also including an engineered air-void system encapsulated within the hydration products to protect the hydration products, and ultimately the concrete, from freezing and thawing damage.

The research used to establish the current air content requirements as espoused in the American Concrete Institute (ACI) Guide to Durable Concrete [2008] was predominantly conducted prior to 1970, and since that time many changes have occurred that significantly affect the quality/characteristics of HCP as well as the entrained air-void system. Some changes that directly impact the quality of HCP include the use of lower water-to-cementitious ratios (w/cm), cements with a finer particle size distribution and an increased C_3S/C_2S ratio, the use of mixtures with lower cementitious material content (CMC), and the extensive use of supplementary cementitious materials SCMs such as fly ash, ground blast furnace slag (slag cement), etc. The biggest change in the characteristics of the entrained air-void system has resulted from the introduction of air entraining agents other than those based on vinsol resins.

For this research, the concrete mixtures prepared were thoroughly characterized, including the measurement of air content, unit weight, air-void system parameters, calorimetric heat signature, absorptivity, F-T performance, maturity, and strength at various ages. Emerging equipment used to measure these properties were also evaluated as part of this research including the Air Void Analyzer (AVA), the Cementometer™, AASHTO T 318 *Standard Method of Test for Water Content of Freshly Mixed Concrete Using Microwave Oven Drying*, and a petrographic-based fluorescent method of w/cm determination. All concrete mixtures were prepared using materials that meet current MDOT specifications.

The research presented here was conducted in three phases. Phase I was a preliminary step to acquire and calibrate equipment evaluated in this research, as described in this report. Phase II was the initial matrix of mixtures tested for the purposes of establishing the properties of the specified mixtures, but also to evaluate equipment as part of this research. Phase III was established after Phase II and was intended to provide a more in-depth understanding of the results obtained in Phase II. To investigate the utility of computer models in the interpretation and prediction of cement paste capillary porosity, selected mixtures were modeled using the National Institute of Standards and Technology (NIST) CEMHYD3D v3.0 Cement Hydration and Microstructure Development Modeling Package [2005].

A total of 148 individual concrete mixtures were produced, and a total of sixteen different tests were performed to characterize and assess the performance of the concrete mixtures. Although

not all of the mixtures were subjected to all sixteen of the tests, in total, the results of well over one thousand tests are summarized within this report.

Overall, the research showed that modern cements and the use of SCMs lead to a hardened cement paste that can potentially have a higher tensile strength and lower permeability. Evidence indicates that the traditional specifications for air content should provide a conservative estimate of performance and incorporating SCMs into concrete mixtures does not necessarily require deviation from these traditional air-void system thresholds. The production of paving concretes with reduced CMC has become more common, and the durability of these concretes, in terms of the laboratory ASTM C666 testing conducted in this study, is superior to the traditional 564 lbs/yd³ CMC concrete, especially for concrete that falls below the 6.5 ± 1.5 vol. % air construction requirement.

There is general agreement between methods of measuring the total air content of a concrete mixture, although the AVA generally does not perform well for this task. With current admixtures, concrete produced with a conventionally accepted level of total air content (e.g. 6.5 ± 1.5 vol. %) can be expected to be F-T durable, but concrete produced with lower air contents can also be durable. The classic limitation of an air-void system spacing factor less than or equal to 0.2 mm is still a safe value to ensure F-T durability, but evidence exists that concrete mixtures with a spacing factor greater than 0.2 mm can also be F-T durable.

Even without detailed measurements of the air void size distribution, the pressure meter air content results and paste content estimates (as computed from the mix design, and defined as the total concrete volume minus the aggregate volume and the air content) perform just as well as the spacing factor calculation at predicting F-T performance.

Test results for water content by AASHTO T 318 compared well with the mixture designs when the measured water content was corrected for aggregate absorption. Test results for w/cm by the Cementometer™ were not as promising, but may be improved with further attention to the calibration process. The petrographic fluorescent method of w/cm determination followed general trends of increased fluorescence intensity with increased w/cm , but exhibited a wide scatter on individual samples and would require standards with similar curing regimes and SCM content for more accurate w/cm determinations. Semi-adiabatic calorimetry proved to be useful tool for identifying delayed-set mixtures. The CEMHYD3D modeling showed the expected pattern of increased porosity for the hydrated systems at elevated w/cm values. The model also predicted the discontinuity of the pore system over a scale of 0.1 mm for the 0.45 w/cm at 25 days. Comparing model output to actual hydrated microstructure shows many similarities, although it is clear that the model does not encompass the finer details of the microstructure due to the limited resolution.

1. Introduction

In cold climates, concrete used in highway infrastructure (e.g. pavements, bridges) is exposed to harsh winter conditions being cyclically frozen and thawed in a saturated state in the presence of chemical deicers. The durability of such concrete is dependent upon many things, including the aggregate component, the hydrated cement paste (HCP) and the presence of a properly entrained air-void system (small, dispersed and closely spaced air bubbles). The research used to establish the current air content requirements as espoused in the American Concrete Institute (ACI) Guide to Durable Concrete [2008] was predominantly conducted prior to 1970, and since that time many changes have occurred that significantly affect the quality/characteristics of HCP as well as the entrained air-void system. Some changes that directly impact the quality of HCP include the use of lower water-to-cementitious ratios (w/cm), cements with a finer particle size distribution, the use of mixtures with lower cementitious material content (CMC), and the extensive use of supplementary cementitious materials (SCMs) such as fly ash, ground blast furnace slag (slag cement), etc. The biggest change in the characteristics of the entrained air-void system has resulted from the introduction of air entraining agents other than those based on vinsol resins.

A major difficulty in predicting the effects to concrete from changes in the HCP quality is that factors contributing to the quality of HCP, including the entrained air-void system, are diverse and not perfectly understood. It is known, for instance, that lowering the w/cm will reduce capillary porosity, therefore increasing strength and reducing the permeability of a given concrete. But how changes in cement fineness and/or chemistry, the presence of various SCMs, and the use of modern air entraining admixtures impacts the freeze-thaw (F-T) durability of HCP is not fully understood.

The entrained air-void system is created through the addition of surface-active agents acting at the water-air interface to create stable foams. Historically, naturally derived vinsol resin-based air entraining admixtures (AEAs) were commonly used and thus specifications for air-entrained concrete are based on these chemicals. As the use of AEAs derived from synthetic or other natural sources increases, changes in the resulting air-void system may make past specification practices incorrect for these concrete mixtures. The issue becomes more clouded in that AEAs may interact in an unexpected manner with other concrete constituents (e.g. cement, SCMs, admixtures), making it difficult to anticipate the quality of the HCP and air-void system in advance of construction.

Although the relationship between the F-T durability of concrete and the quality of the hydrated cement paste and the air-void system are thought to be well established, there have been sufficient changes in concrete mixtures (e.g. lower w/cm , the use of SCMs, synthetic versus vinsol resin AEAs, lower CMC, etc.) and problems in the field to warrant a study to re-examine the accepted relationships.

2. Objective

In cold climates, concrete used in pavements and bridges must be able to withstand cyclic freezing and thawing. Durability in these environments is achieved through the production of air-entrained concrete. Admixtures used to achieve an air-void system have changed and current concrete mixtures use more SCMs. This study is designed to examine whether traditional limits used to describe the air-void system still apply to concrete prepared with these new admixtures and materials. This report describes the production, characterization, and F-T testing of a series of laboratory concrete mixtures that represent a variety of HCPs and air-void systems. In addition, this report utilizes newly available test equipment to assess the w/cm and air-void system in fresh concrete. Based on the results of this research, recommendations will be made to improve the F-T durability and cost effectiveness of concrete mixtures currently being used in Michigan. Furthermore, recommendations will be made regarding potential implementation of new test equipment to improve construction quality control and quality assurance.

3. Scope

Overall this research examines the relationship(s) between F-T durability and the quality of HCP, including the air-void system parameters, for various concrete mixtures. The concrete mixtures prepared were thoroughly characterized, including the measurement of air content, unit weight, air-void system parameters, calorimetric heat signature, absorptivity, F-T performance, maturity, and strength at various ages. This report also examines the performance of new analytical equipment and techniques for concrete characterization.

4. Methodology

4.1 Mixture Design Experimental Matrices

4.1.1 Phase II Mixtures

The research presented here was conducted in three phases. Phase I was a preliminary step to acquire and calibrate equipment evaluated in this research, as described in this report. Phase II was the initial matrix of mixtures tested for the purposes of establishing the properties of the specified mixtures, but also to evaluate equipment as part of this research. Phase III was established after Phase II and was intended to provide a more in-depth understanding of the results obtained in Phase II

To accomplish Phase II of the research, a combined full and partial-factorial experimental matrix was established that resulted in a total of 68 different concrete mixtures. Each mixture was prepared in duplicate. The mixture parameters used are shown in Table 1 and included:

- Two target air contents: 3 ± 1 vol. % and 6.5 ± 1.5 vol. %.
- AEAs: one vinsol resin and one synthetic.
- SCMs: none, fly ash (25 wt. % replacement level), slag cement (40 wt. % replacement level).
- CMCs: 470 lbs/yd³, 517 lbs/yd³, and 564 lbs/yd³.
- Target w/cm : 0.45, 0.50, and 0.52.

Table 1: Phase II mixture design experimental matrix.

Mixture ID	Target Air Content vol. %	AEA Type	CMC sacks/yd ³	Target w/cm	Mix Design w/cm	Air Entrainer fl. oz/cwt	Water Reducer	Aggregate					
								Water	Portland Cement	Fly Ash	Slag Cement	Fine	
HI-VR-PC-6SK-45WC	6.5	vinsol	6	0.45	0.46	2.1	4.5	253.8	564.0	0.0	0.0	1638.8	1379.5
HI-SYN-PC-6SK-45WC	6.5	syn.	6	0.45	0.45	1.9	3.0	253.8	564.0	0.0	0.0	1638.8	1381.1
HI-VR-SLG-6SK-45WC	6.5	vinsol	6	0.45	0.46	2.1	4.5	253.8	338.4	0.0	22.5.6	1638.8	1363.1
HI-SYN-SLG-6SK-45WC	6.5	syn.	6	0.45	0.45	0.8	3.0	253.8	338.4	0.0	22.5.6	1638.8	1365.8
HI-VR-FA-6SK-45WC	6.5	vinsol	6	0.45	0.45	1.7	0.7	253.8	423.0	141.0	0.0	1638.8	1358.4
HI-SYN-FA-6SK-45WC	6.5	syn.	6	0.45	0.45	1.5	0.4	253.8	423.0	141.0	0.0	1638.8	1358.9
HI-VR-PC-5SK-45WC	6.5	vinsol	5	0.45	0.46	2.2	11.3	211.5	470.0	0.0	0.0	1760.0	1447.7
HI-SYN-PC-5SK-45WC	6.5	syn.	5	0.45	0.46	3.8	12.1	211.5	470.0	0.0	0.0	1760.0	1445.8
HI-VR-SLG-5SK-45WC	6.5	vinsol	5	0.45	0.46	0.8	13.6	211.5	282.0	0.0	188.0	1750.0	1443.5
HI-SYN-SLG-5SK-45WC	6.5	syn.	5	0.45	0.46	0.8	13.6	211.5	282.0	0.0	188.0	1750.0	1443.5
HI-VR-PC-6SK-50WC	6.5	vinsol	6	0.50	0.50	0.7	0.0	282.0	564.0	0.0	0.0	1638.8	1310.5
HI-SYN-PC-6SK-50WC	6.5	syn.	6	0.50	0.50	0.6	0.0	282.0	564.0	0.0	0.0	1638.8	1310.6
HI-VR-SLG-6SK-50WC	6.5	vinsol	6	0.50	0.50	0.4	0.0	282.0	338.4	0.0	22.5.6	1638.8	1294.4
HI-VR-PC-5.5SK-52WC	6.5	vinsol	5.5	0.52	0.52	0.7	0.0	268.8	517.0	0.0	0.0	1638.8	1384.9
HI-SYN-PC-5.5SK-52WC	6.5	syn.	5.5	0.52	0.52	0.4	0.0	268.8	517.0	0.0	0.0	1638.8	1385.2
HI-VR-SLG-5.5SK-52WC	6.5	vinsol	5.5	0.52	0.52	0.9	0.0	268.8	310.2	0.0	206.8	1638.8	1369.7
HI-SYN-SLG-5.5SK-52WC	6.5	syn.	5.5	0.52	0.52	0.9	0.0	268.8	310.2	0.0	206.8	1638.8	1369.7
LO-VR-PC-6SK-45WC	3	vinsol	6	0.45	0.46	1.0	4.5	253.8	564.0	0.0	0.0	1638.8	1514.4
LO-SYN-PC-6SK-45WC	3	syn.	6	0.45	0.46	0.9	4.5	253.8	564.0	0.0	0.0	1638.8	1514.6
LO-VR-SLG-6SK-45WC	3	vinsol	6	0.45	0.46	1.1	4.5	253.8	338.4	0.0	22.5.6	1638.8	1498.0
LO-SYN-SLG-6SK-45WC	3	syn.	6	0.45	0.46	0.2	4.5	253.8	338.4	0.0	22.5.6	1638.8	1498.9
LO-VR-FA-6SK-45WC	3	vinsol	6	0.45	0.45	0.3	1.1	253.8	423.0	141.0	0.0	1638.8	1493.4
LO-SYN-FA-6SK-45WC	3	syn.	6	0.45	0.45	0.2	1.1	253.8	423.0	141.0	0.0	1638.8	1493.4
LO-VR-PC-5SK-45WC	3	vinsol	5	0.45	0.48	0.5	13.2	211.5	470.0	0.0	0.0	1835.0	1505.5
LO-SYN-PC-5SK-45WC	3	syn.	5	0.45	0.48	0.2	14.3	211.5	470.0	0.0	0.0	1835.0	1504.8
LO-VR-SLG-5SK-45WC	3	vinsol	5	0.45	0.48	0.1	15.1	211.5	282.0	0.0	188.0	1825.0	1500.8
LO-SYN-SLG-5SK-45WC	3	syn.	5	0.45	0.48	0.1	12.8	211.5	282.0	0.0	188.0	1825.0	1502.7
LO-VR-PC-6SK-50WC	3	vinsol	6	0.50	0.50	0.3	0.0	282.0	564.0	0.0	0.0	1638.8	1444.8
LO-SYN-PC-6SK-50WC	3	syn.	6	0.50	0.50	0.3	0.0	282.0	564.0	0.0	0.0	1638.8	1444.8
LO-VR-SLG-6SK-50WC	3	vinsol	6	0.50	0.50	0.3	0.0	282.0	338.4	0.0	22.5.6	1638.8	1428.4
LO-VR-PC-5.5SK-52WC	3	vinsol	5.5	0.52	0.52	0.3	0.0	268.8	517.0	0.0	0.0	1638.8	1519.3
LO-SYN-PC-5.5SK-52WC	3	syn.	5.5	0.52	0.52	0.2	0.0	268.8	517.0	0.0	0.0	1638.8	1519.3
LO-VR-SLG-5.5SK-52WC	3	vinsol	5.5	0.52	0.52	0.1	0.0	268.8	310.2	0.0	206.8	1638.8	1504.4
LO-SYN-SLG-5.5SK-52WC	3	syn.	5.5	0.52	0.52	0.2	0.0	268.8	310.2	0.0	206.8	1638.8	1504.3

The mixture identification used throughout this report indicates the key properties of each mixture by using the following codes:

Target Air Content	HI	6.5 vol. %
	LO	3 vol. %
	VLO	2 vol. %
AEA Type	VR	vinsol resin
	SYN	synthetic
Cementitious Material	PC	portland cement only
	FA	25 wt. % replacement level
	SLG	40 wt. % replacement level
CMC	xSK where x = number of sacks per cubic yard (i.e. 1 sack = 94 lb)	
Water-cementitious ratio	yWC where y = target w/cm *100	

Example: The mixture ID LO-SYN-PC-5.5SK-52WC represents a mixture with a 3 vol. % target air content, synthetic AEA, portland cement only, 5.5 sacks of cementitious material per cubic yard (517 lbs.yd³), and a target w/cm of 0.52.

4.1.2 Phase III Mixtures

In Phase III of the research, an additional full experimental matrix of 12 different mixtures was designed to explore concrete with very low air contents (2 ± 1 vol. % air) and a w/cm of 0.46. The mixture parameters used are shown in Table 2 and included:

- AEA: one vinsol resin and one synthetic.
- SCMs: none, fly ash (25 wt. % replacement level), slag cement (40 wt. % replacement level).
- CMCs: 564 lbs/yd³, 490 lbs/yd³.

4.2 Materials

4.2.1 Physical Properties of Materials

The following materials were used to produce the concrete mixtures. Table 3 summarizes the physical properties of the materials used.

- Lafarge Type I/II portland cement from the Alpena, Michigan plant.
- Holcim Class C fly ash from the Detroit Edison Belle River 1 near St. Clair, Michigan.
- Lafarge NewCem[®] Grade 120 slag cement.
- Coarse aggregate from the Presque Isle limestone quarry near Alpena, Michigan.
- Fine aggregate from the Lindberg Co. Rd. 480 pit near Marquette, Michigan, and fine aggregate from the Superior Sand & Gravel pit near Hancock, Michigan.
- Master Builders MicroAir[®] AEA.
- Master Builders MB VR Standard[®] AEA.
- Master Builders Polyheed 997[®] mid-range water reducing admixture.

Table 2: Phase III mixture design experimental matrix.

Mixture ID	Target Air Content vol. %	AEA Type	CMC sacks/yard ³	Target w/cm	Mix Design w/cm	Air Entrainer fl. oz/cwt	Water Reducer	Water	Portland Cement	Fly Ash	Slag Cement	Aggregate	
												Coarse	Fine
VLO-VR-PC-6SK-46WC	2	vinsol	6	0.46	0.46	0.06	9.0	255.2	564.0	0.0	0.0	1599.6	1536.8
VLO-SYN-PC-6SK-46WC	2	syn.	6	0.46	0.46	0.03	9.0	255.2	564.0	0.0	0.0	1599.6	1536.8
VLO-VR-SLG-6SK-46WC	2	vinsol	6	0.46	0.46	0.06	9.0	255.2	338.4	0.0	225.6	1591.4	1529.0
VLO-SYN-SLG-6SK-46WC	2	syn.	6	0.46	0.46	0.03	9.0	255.2	338.4	0.0	225.6	1591.4	1529.0
VLO-VR-FA-6SK-45WC	2	vinsol	6	0.46	0.46	0.06	0.0	259.4	423.0	141.0	0.0	1616.2	1491.9
VLO-SYN-FA-6SK-46WC	2	syn.	6	0.46	0.46	0.03	0.0	259.4	423.0	141.0	0.0	1616.2	1491.9
VLO-VR-PC-5.2SK-46WC	2	vinsol	5.2	0.46	0.46	0.06	9.0	221.7	490.0	0.0	0.0	1717.9	1585.8
VLO-SYN-PC-5.2SK-46WC	2	syn.	5.2	0.46	0.46	0.03	9.0	221.7	490.0	0.0	0.0	1717.9	1585.8
VLO-VR-SLG-5.2SK-46WC	2	vinsol	5.2	0.46	0.46	0.06	12.0	220.5	294.0	0.0	196.0	1711.0	1579.4
VLO-SYN-SLG-5.2SK-46WC	2	syn.	5.2	0.46	0.46	0.03	12.0	220.5	294.0	0.0	196.0	1711.0	1579.4
VLO-VR-FA-5.2SK-46WC	2	vinsol	5.2	0.46	0.46	0.06	3.0	224.2	367.5	122.5	0.0	1706.1	1574.9
VLO-SYN-FA-5.2SK-46WC	2	syn.	5.2	0.46	0.46	0.03	3.0	224.2	367.5	122.5	0.0	1706.1	1574.9

Table 3: Physical properties of materials.

	Material	Bulk Specific Gravity	Absorption (wt. %)
Cementitious components	Lafarge Type I/II portland cement	3.15	
	Holcim Class C fly ash	2.60	
	Lafarge NewCem [®] slag cement	2.90	
Phase II aggregate sources	Presque Isle limestone, MDOT 6A/6AA	2.53	1.88
	Presque Isle limestone, optimized gradation	2.53	1.94
	Lindberg Co. Rd. 480, MDOT 2NS	2.67	1.01
	Superior S&G, MDOT 2NS	2.64	1.36
Phase III aggregate sources	Presque Isle limestone, MDOT 6A/6AA	2.55	2.01
	Presque Isle limestone, optimized gradation	2.55	2.01
	Superior S&G, MDOT 2NS	2.65	0.87

4.2.2 Aggregate Gradations

Figure 1 shows the fine aggregate gradations used to produce the Phase II and Phase III mixtures. The Phase II 517 lbs/yd³ and 564 lbs/yd³ CMC mixtures used fine aggregate from the Lindberg Co. Rd. 480 pit, while the Phase II 470 lbs/yd³ CMC mixtures used fine aggregate from the Superior Sand & Gravel pit. All Phase III mixtures used fine aggregate from the Superior Sand & Gravel pit. The change in fine aggregate source was done simply to facilitate procurement (i.e. the Superior Sand & Gravel pit is in the Houghton area). A petrographic examination and sieve analysis was performed to confirm the similarity between the two sources. From a mineralogical perspective, they were quite similar both being glacial sands. In terms of grading, the differences were insignificant. The 517 lbs/yd³ and 564 lbs/yd³ CMC mixtures from both Phase II and Phase III used an MDOT 6A/6AA gradation coarse aggregate produced at the Presque Isle limestone quarry, as shown in Figure 2.

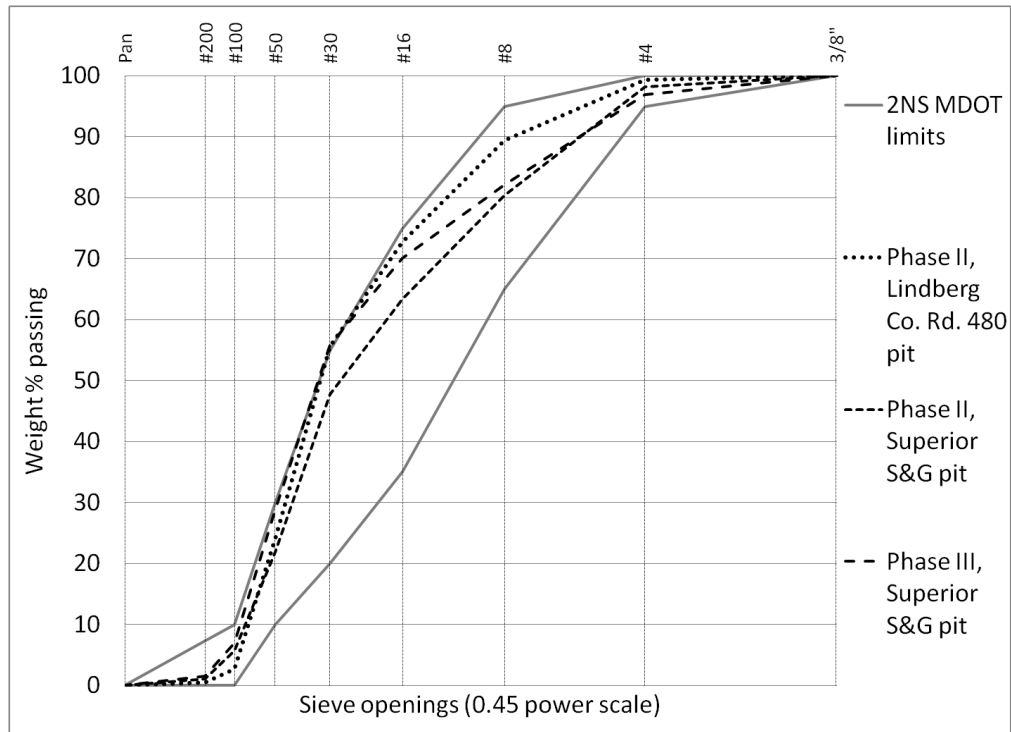


Figure 1: MDOT 2NS gradation limits and as-received fine aggregate gradations from Superior S&G pit and Lindberg Co. Rd. 480 pit.

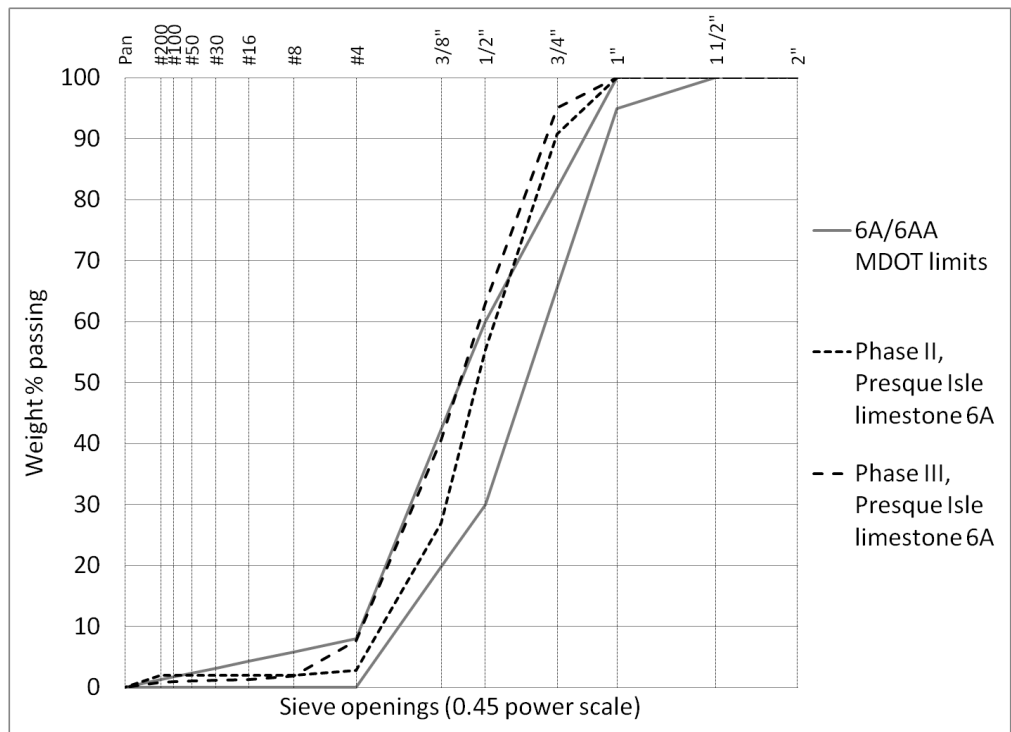


Figure 2: MDOT 6A/6AA gradation limits and as-received coarse aggregate gradations from Presque Isle limestone quarry.

Figure 3 shows the coarse aggregate gradations used to produce the 470 lbs/yd³ and 490 lbs/yd³ CMC concrete mixtures. Both the Phase II 470 lbs/yd³ CMC mixtures and the Phase III 490

lbs/yd³ CMC mixtures used coarse aggregate from the Presque Isle limestone quarry. The MDOT gradation limits shown on Figures 2 and 3 require a minimum percentage of material to be retained on the 1-inch sieve. However, the dimensions of the molds used for the laboratory hardened concrete test specimens precluded the use of a 1-inch top size aggregate, and thus a 3/4-inch top size was used for all concrete mixtures.

Figure 4 plots the combined aggregate gradation for the 517 lbs/yd³ and 564 lbs/yd³ CMC mixtures on a percent retained chart (i.e. “haystack” chart). Figure 5 plots the location of the combined aggregate gradations on a Shilstone coarseness factor - workability factor (CF/WF) chart (Shilstone 1990). For the Phase II high air content target concrete mixtures (6.5 vol. % air) the coarse and fine aggregates were combined together at a ratio of approximately 55/45 by weight. For the Phase II low air content target concrete mixtures (3 vol. % air) and the Phase III very low air content target concrete mixtures (2 vol. % air) the coarse and fine aggregate were combined at a ratio of approximately 52/48, coarse to fine respectively, by weight. In most cases the absolute ratio of coarse to fine aggregate was varied slightly depending on the specifics of the concrete mixture (i.e. *w/cm*, SCM content) in an effort to maintain workable mixtures.

Figure 6 plots the combined aggregate gradation for the 470 lbs/yd³ and 490 lbs/yd³ CMC mixtures on a haystack chart, and Figure 7 plots the location of the combined aggregate gradations on a Shilstone CF/WF chart. For all Phase II 470 lbs/yd³ CMC concrete mixtures the coarse and fine aggregate were combined at a ratio of approximately 55/45 by weight. For the Phase III 490 lbs/yd³ CMC concrete mixtures the coarse and fine aggregate were combined at a ratio of approximately 52/48 by weight. The recommended limits shown in Figures 4-7 reflect the MDOT Special Provision for High Performance Portland Cement Concrete Grade P1 (Modified).

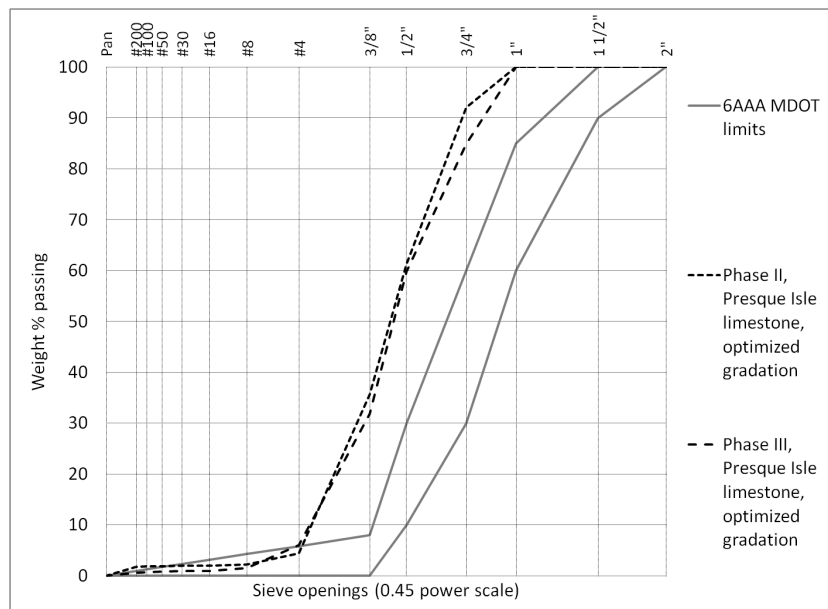


Figure 3: MDOT 6AAA gradation limits and manufactured optimized coarse aggregate gradations from Presque Isle limestone.

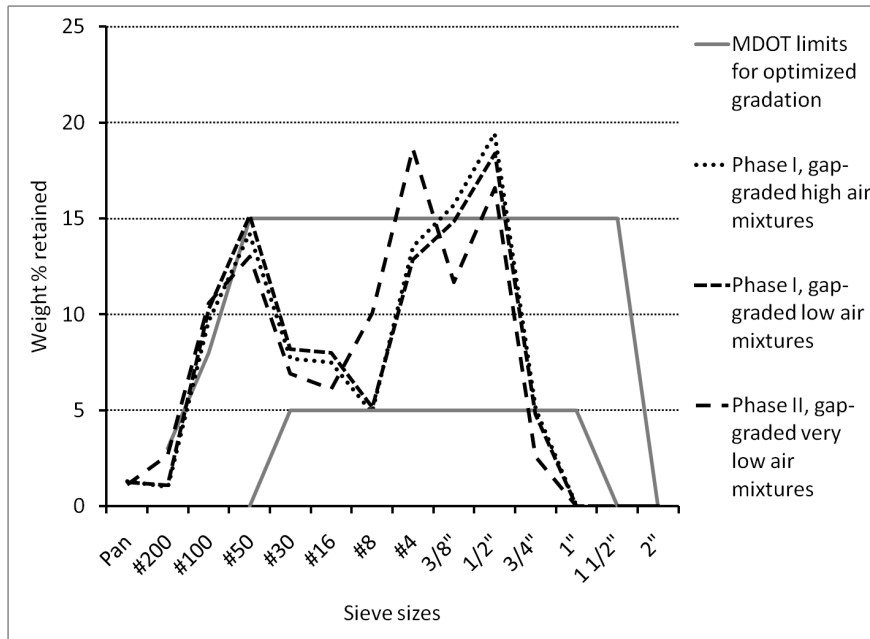


Figure 4: Percent retained “haystack” chart with recommended MDOT optimized gradation limits, and combined aggregate gradations for the gap-graded concrete mixtures.

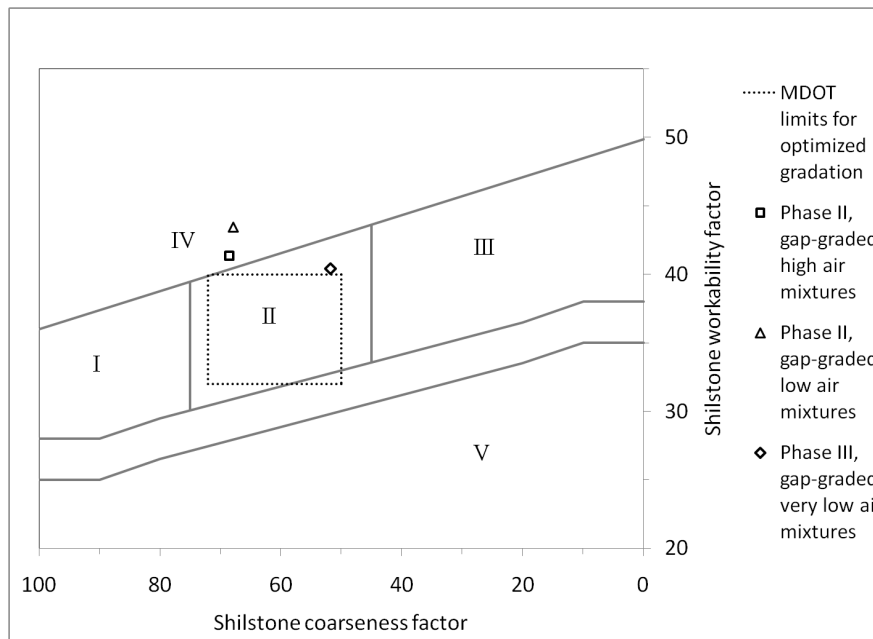


Figure 5: Shilstone coarseness factor - workability factor chart with recommended MDOT optimized gradation limits, and locations of the gap-graded concrete mixtures. Roman numerals I-V indicate zones of predicted properties (Richardson, 2005): (I) – coarse, gap graded, (II) – well-graded 1 – 1-1/2 inch top-size, (III) - well-graded minus 3/4 inch top-size, inch top-size, (IV) – over-sanded, (V) – rocky.

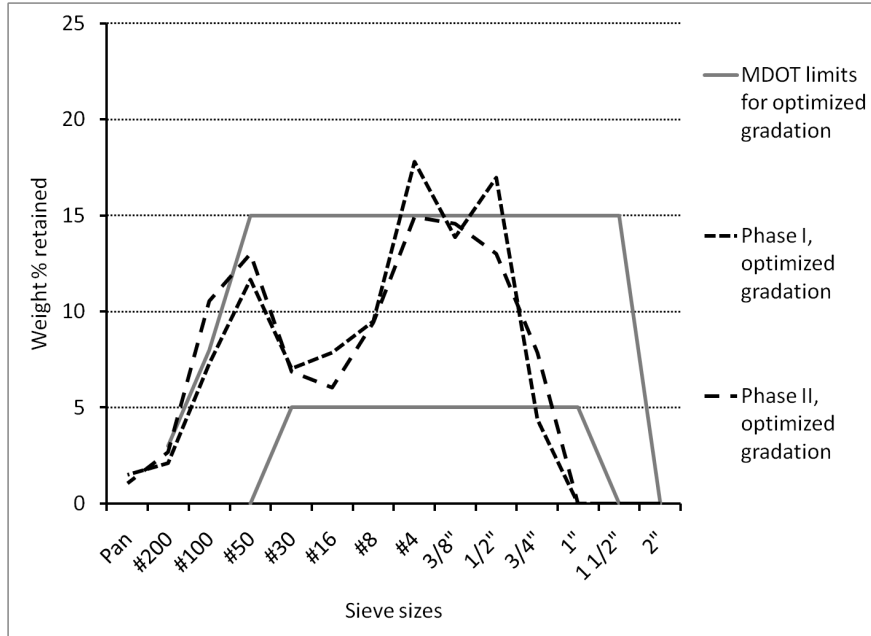


Figure 6: Percent retained “haystack” chart with recommended MDOT optimized gradation limits, and combined aggregate gradations for the optimized concrete mixtures.

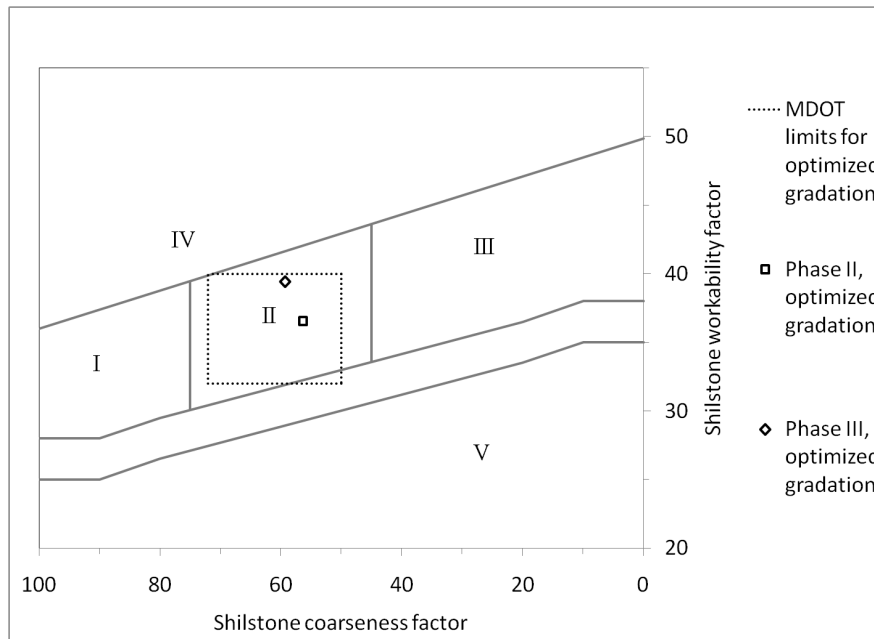


Figure 7: Shilstone coarseness factor - workability factor chart with recommended MDOT optimized gradation limits, and locations of the optimized concrete mixtures. Roman numerals refer to Shilstone. Roman numerals I-V indicate zones of predicted properties (Richardson, 2005): (I) – coarse, gap graded, (II) – well-graded 1 – 1-1/2 inch top-size, (III) - well-graded minus 3/4 inch top-size, (IV) – over sanded, (V) – rocky.

5. Test Results

5.1 Fresh Concrete Tests

5.1.1 Standard Fresh Concrete Tests

A variety of fresh concrete tests were performed to assess the quality of the mixtures, including:

- ASTM C1064 Standard Test Method for Temperature of Freshly Mixed Hydraulic-Cement Concrete.
- ASTM C143 Standard Test Method for Slump of Hydraulic-Cement Concrete.
- ASTM C173 Standard Test Method for Air Content of Freshly Mixed Concrete by the Volumetric Method.
- ASTM C231 Standard Test Method for Air Content of Freshly Mixed Concrete by the Pressure Method.
- ASTM C138 Standard Test Method for Density (Unit Weight), Yield, and Air Content (Gravimetric) of Concrete.
- AASHTO T 318 Standard Method of Test for Water Content of Freshly Mixed Concrete Using Microwave Oven Drying.

The fresh concrete tests results for the Phase II high air content and low air content mixtures are summarized in Tables 4 and 5. The fresh concrete tests results for the Phase III very low air content mixtures are summarized in Table 6. The AVA-3000, Cementometer™, and AASHTO T 318 microwave oven drying test was not performed on any Phase III mixtures given that Phase II was focused on the performance of the mixtures, not to further evaluate emerging equipment. Figures 8-12 plot the results of slump tests for all Phase III mixtures. Figure 13 plots the results of pressure meter air content tests.

5.1.2 Additional Fresh Concrete Tests

In addition to the standard tests, the following fresh-concrete tests were also performed on the Phase II mixtures:

- Air-void system parameters of fresh concrete using a Germann Instruments AVA-3000.
- Semi-adiabatic calorimetry using a Grace Adiacal™.
- w/cm ratio using a James Cementometer™ Type R microwave moisture meter.

The AVA-3000 air-void parameters and Cementometer™ w/cm readings are included in Tables 4 and 5, calorimetry curves are included in Figures 14-17.

Table 4: Fresh concrete test results and air-void parameters for Phase II high air-content mixtures.

Mixture ID	Concrete Temp °F	Slump (in.)	Unit Weight (lbs/ft ³)	AASHTO T 318 (lbs/yd ³)	Cement-ometer w/cm	Air Content (vol.%)				Specific Surface		Spacing Factor			
						ASTM C231	ASTM C173	ASTM C138	AVA	Flatbed Scanner	AVA (mm ⁻¹)	Flatbed Scanner	AVA (mm)	Flatbed Scanner	AVA (mm)
HI-VR-PC-6SK-45WC	70	4.00	141.9	264.2	0.46	7.2	6.2	6.2	4.0	7.1	29.4	31.5	0.194	0.107	
	70	2.50	145.0	270.9	0.46	6.3	5.2	4.2	3.4	6.2	33.4	24.2	0.184	0.160	
HI-SYN-PC-6SK-45WC	72	2.00	146.2	258.8	0.43	5.3	5.5	3.4	3.0	5.5	30.2	20.7	0.217	0.211	
	72	2.50	145.1	258.5	0.44	5.7	6.2	4.2	3.2	5.0	28.7	28.1	0.221	0.163	
HI-VR-SLG-6SK-45WC	67	4.75	140.5	247.3	0.44	7.2	7.0	6.8	5.1	7.1	29.0	27.9	0.178	0.123	
	67	4.75	141.7	275.4	0.44	6.9	6.7	6.0	8.9	7.2	31.1	24.4	0.116	0.137	
HI-SYN-SLG-6SK-45WC	70	5.75	145.8	257.3	0.45	5.4	6.2	3.3	3.3	5.4	27.8	24.5	0.225	0.181	
	70	4.75	145.7	270.2	0.46	5.7	5.2	3.4	3.0	6.0	30.8	21.6	0.212	0.189	
HI-VR-FA-6SK-45WC	79	3.25	143.3	225.4	0.45	6.5	7.5	4.8	4.0	7.0	27.9	20.4	0.198	0.169	
	79	4.25	141.9	211.8	0.50	7.4	5.7	5.7	4.6	8.8	29.5	27.3	0.176	0.098	
HI-SYN-FA-6SK-45WC	80	3.50	139.3	231.3	0.41	8.0	6.7	7.5	-0.5	8.2	-56.1	35.3	1.079	0.082	
	80	3.75	140.6	232.9	0.41	7.7	6.5	6.6	6.0	7.0	46.2	36.9	0.104	0.094	
HI-VR-PC-5SK-45WC	74	1.00	141.8	193.0	-	8.9	5.2	7.7	1.7	11.5	11.7	25.3	0.667	0.065	
	74	0.25	144.5	197.6	-	7.4	4.0	5.9	1.6	9.4	12.4	21.0	0.662	0.098	
HI-SYN-PC-5SK-45WC	74	0.75	143.1	208.1	0.41	7.7	5.5	6.8	2.9	7.4	42.0	28.0	0.149	0.094	
	75	0.50	144.9	198.4	0.40	6.7	6.0	5.6	5.7	7.3	26.1	24.8	0.176	0.108	
HI-VR-SLG-5SK-45WC	72	1.25	141.8	206.8	0.41	7.8	7.2	7.3	5.8	8.3	36.5	21.1	0.125	0.113	
	72	1.00	144.2	210.4	0.43	6.6	6.0	5.8	4.4	5.6	37.0	22.7	0.140	0.159	
HI-SYN-SLG-5SK-45WC	62	0.75	146.6	202.1	0.38	5.7	5.5	4.2	4.0	5.4	43.5	28.6	0.124	0.132	
	63	1.50	143.2	209.2	0.43	7.5	7.7	6.4	5.3	6.8	42.7	31.3	0.111	0.094	
HI-VR-PC-6SK-50WC	72	4.75	144.4	296.8	0.52	5.4	5.5	3.5	3.5	6.9	25.3	21.5	0.244	0.168	
	74	7.00	143.3	304.9	0.51	5.7	6.5	4.3	6.1	5.6	43.6	23.1	0.110	0.191	
HI-SYN-PC-6SK-50WC	66	7.25	142.1	278.6	0.50	7.1	7.2	5.1	5.1	5.8	25.8	29.4	0.203	0.147	
	66	6.50	143.9	281.6	0.50	5.8	7.7	3.9	4.2	7.3	25.7	22.7	0.222	0.149	
HI-VR-SLG-6SK-50WC	63	7.50	144.1	280.4	0.52	4.8	5.2	3.3	3.2	5.2	24.8	22.0	0.261	0.210	
	65	8.00	145.4	284.4	0.51	4.6	5.0	2.5	3.0	4.2	24.2	27.0	0.278	0.189	
HI-VR-PC-5.5SK-52WC	74	5.25	144.0	265.3	0.51	5.8	5.5	4.2	3.3	6.6	22.5	19.5	0.232	0.184	
	74	3.50	143.7	278.6	0.51	5.7	6.0	4.4	3.6	6.4	23.0	20.6	0.220	0.181	
HI-SYN-PC-5.5SK-52WC	74	2.75	144.7	282.0	0.52	3.9	5.2	3.7	3.5	6.5	29.5	19.0	0.207	0.193	
	74	3.25	144.4	280.2	0.52	4.2	5.5	3.9	3.8	6.5	32.4	18.5	0.181	0.198	
HI-VR-SLG-5.5SK-52WC	71	4.50	142.9	276.9	0.43	6.1	6.0	4.5	3.8	5.3	26.0	23.0	0.227	0.193	
	72	3.50	144.4	255.3	0.45	5.5	5.5	3.5	3.2	5.5	26.0	24.6	0.244	0.178	
HI-SYN-SLG-5.5SK-52WC	77	3.75	144.4	268.3	0.46	5.0	5.2	3.5	3.2	4.5	28.6	25.4	0.221	0.190	
	77	3.50	144.2	265.8	0.47	4.8	5.2	3.7	3.3	4.4	25.4	25.3	0.247	0.192	

Table 5: Fresh concrete test results and air-void parameters for Phase II low air-content mixtures.

Mixture ID	Concrete Temp °F	Slump (in.)	Unit Weight (lbs/ft ³)	AASHTO T 318 (lbs/ft ³)	Cement-ometer w/cm	Air Content (vol.%)						Specific Surface		Spacing Factor	
						ASTM C231	ASTM C173	ASTM C138	AVA	Flatbed Scanner	AVA (mm ⁻¹)	Flatbed Scanner	AVA (mm)	Flatbed Scanner	
LO-VR-PC-6SK-45WC	70	1.00	147.3	247.0	0.42	3.5	2.7	2.9	2.9	5.0	15.0	13.2	0.417	0.350	
	70	0.75	147.3	247.0	0.43	3.7	2.7	2.9	3.1	4.2	9.7	18.5	0.629	0.268	
LO-SYN-PC-6SK-45WC	72	0.75	147.5	247.8	0.41	3.9	4.0	2.9	2.3	4.8	26.6	19.4	0.265	0.240	
	72	1.25	147.3	260.7	0.41	4.1	4.0	3.0	2.4	6.6	20.6	16.1	0.334	0.225	
LO-VR-SLG-6SK-45WC	68	1.75	148.4	247.9	0.42	3.5	3.5	1.9	2.1	3.5	18.9	20.2	0.390	0.272	
	67	2.00	147.2	258.8	0.41	3.5	4.0	2.7	2.1	5.1	21.5	12.4	0.344	0.368	
LO-SYN-SLG-6SK-45WC	78	1.25	148.7	262.9	0.42	3.2	2.2	1.7	-1.3	3.5	6.4	10.8	-3.586	0.507	
	79	1.00	147.8	246.7	0.42	3.0	1.2	2.3	1.4	5.3	26.1	11.3	0.334	0.397	
LO-VR-FA-6SK-45WC	79	1.25	149.6	223.4	0.48	2.8	3.2	0.9	1.0	5.7	35.7	11.7	0.276	0.369	
	79	1.75	149.5	235.7	0.46	3.0	2.7	1.0	2.2	4.2	19.3	16.4	0.362	0.305	
LO-SYN-FA-6SK-45WC	80	2.50	148.2	220.9	0.40	3.5	3.5	1.8	1.8	4.1	21.8	18.9	0.364	0.268	
	80	2.25	148.4	235.5	0.43	3.4	3.5	1.7	0.8	5.7	71.3	18.0	0.152	0.240	
LO-VR-PC-5SK-45WC	74	0.50	149.1	204.2	-	5.5	4.2	3.1	0.0	5.8	-1054.4	19.7	0.580	0.169	
	74	1.00	147.4	201.3	-	5.6	4.7	4.2	0.0	6.9	45.8	20.2	0.697	0.136	
LO-SYN-PC-5SK-45WC	75	0.00	151.0	221.1	0.39	3.1	3.7	1.9	1.0	4.8	21.3	15.7	0.433	0.260	
	74	0.00	149.6	191.6	0.41	3.4	3.7	2.8	1.1	5.0	37.0	18.5	0.246	0.211	
LO-VR-SLG-5SK-45WC	80	0.75	149.1	216.8	0.42	3.4	4.0	2.8	2.6	4.6	20.3	15.4	0.309	0.279	
	81	0.00	151.1	207.7	0.43	2.2	2.2	1.5	1.5	3.6	21.6	14.5	0.363	0.338	
LO-SYN-SLG-5SK-45WC	63	0.50	148.7	190.3	0.43	4.0	3.5	3.1	2.9	5.7	34.1	15.0	0.175	0.230	
	64	0.50	150.4	206.5	0.43	3.6	4.0	2.0	5.7	4.4	44.4	16.3	0.098	0.271	
LO-VR-PC-6SK-50WC	70	3.00	147.7	288.8	0.49	3.0	2.5	1.7	2.1	5.4	17.5	13.1	0.427	0.342	
	71	3.50	147.2	288.8	0.50	3.0	3.0	2.0	2.0	4.7	18.9	15.7	0.403	0.308	
LO-SYN-PC-6SK-50WC	69	2.75	148.4	277.1	0.42	3.3	3.5	1.2	1.8	5.4	19.4	13.9	0.409	0.323	
	69	3.50	148.0	276.2	0.46	3.4	3.7	1.5	3.8	6.1	12.8	20.9	0.448	0.198	
LO-VR-SLG-6SK-50WC	65	7.75	146.1	308.7	0.46	4.1	4.0	2.3	2.5	3.9	22.6	21.8	0.306	0.244	
	63	8.00	145.4	283.1	0.47	4.7	4.5	2.8	3.0	4.2	23.8	24.0	0.269	0.212	
LO-VR-PC-5.5SK-52WC	72	3.00	148.0	259.2	0.51	3.0	3.2	1.8	2.9	5.6	13.2	9.7	0.566	0.441	
	72	2.75	147.4	260.0	0.44	3.4	3.2	2.2	2.3	4.6	14.5	14.4	0.488	0.330	
LO-SYN-PC-5.5SK-52WC	74	2.25	148.0	275.8	0.48	2.8	3.7	1.8	2.7	4.4	29.2	16.5	0.223	0.294	
	74	2.50	147.5	272.7	0.48	2.9	3.2	2.1	3.2	4.8	30.0	16.7	0.230	0.278	
LO-VR-SLG-5.5SK-52WC	71	1.25	146.7	257.7	-	2.7	2.7	2.3	2.3	3.1	11.6	18.8	0.602	0.304	
	71	2.50	148.0	273.7	0.41	2.9	3.0	1.4	1.7	4.9	15.3	13.8	0.526	0.338	
LO-SYN-SLG-5.5SK-52WC	76	1.25	148.2	248.5	0.44	3.5	2.7	1.3	3.2	4.4	20.0	12.8	0.304	0.379	
	76	1.00	146.9	257.1	0.44	2.9	2.7	2.2	1.6	4.1	17.2	15.9	0.476	0.318	

Table 6: Fresh concrete test results and air-void parameters for Phase III very low air-content mixtures.

Mixture ID	Concrete Temp °F	Slump (in.)	Unit Weight (lbs/ft ³)	AASHTO T 318 (lbs/yd ³)	Cement-ometer w/cm	Air Content (vol.%)				Specific Surface		Spacing Factor		
						ASTM C231	ASTM C173	ASTM C138	AVA	Flatbed Scanner	AVA (mm ⁻¹)	Flatbed Scanner	AVA (mm)	Flatbed Scanner
VLO-VR-PC-6SK-46WC	70	1.50	145.8	-	-	3.6	3.3	3.7	-	3.8	-	17.5	-	0.301
VLO-SYN-PC-6SK-46WC	63	1.25	146.2	-	-	3.5	4.0	3.4	-	4.4	-	14.6	-	0.337
VLO-VR-SLG-6SK-46WC	60	0.75	146.2	-	-	3.1	3.5	3.0	-	4.5	-	12.0	-	0.410
VLO-SYN-SLG-6SK-46WC	60	0.75	146.2	-	-	3.4	3.5	3.0	-	3.6	-	10.4	-	0.523
VLO-VR-FA-6SK-45WC	70	2.25	148.0	-	-	2.3	2.5	1.5	-	3.1	-	10.5	-	0.556
VLO-SYN-FA-6SK-46WC	70	2.25	148.0	-	-	2.3	2.5	1.5	-	2.4	-	10.5	-	0.627
VLO-VR-PC-5.2SK-46WC	60	0.75	147.2	-	-	4.0	4.0	4.2	-	4.9	-	11.8	-	0.371
VLO-SYN-PC-5.2SK-46WC	61	0.25	149.4	-	-	3.3	3.5	2.8	-	3.6	-	13.3	-	0.382
VLO-VR-SLG-5.2SK-46WC	60	0.25	147.6	-	-	3.6	3.8	3.7	-	3.9	-	12.1	-	0.407
VLO-SYN-SLG-5.2SK-46WC	58	0.25	148.0	-	-	3.8	3.8	3.4	-	2.9	-	14.3	-	0.400
VLO-VR-FA-5.2SK-46WC	57	0.25	148.8	-	-	3.0	3.3	2.7	-	6.2	-	7.5	-	0.471
VLO-SYN-FA-5.2SK-46WC	62	1.00	148.6	-	-	3.3	3.3	2.8	-	5.1	-	7.2	-	0.608

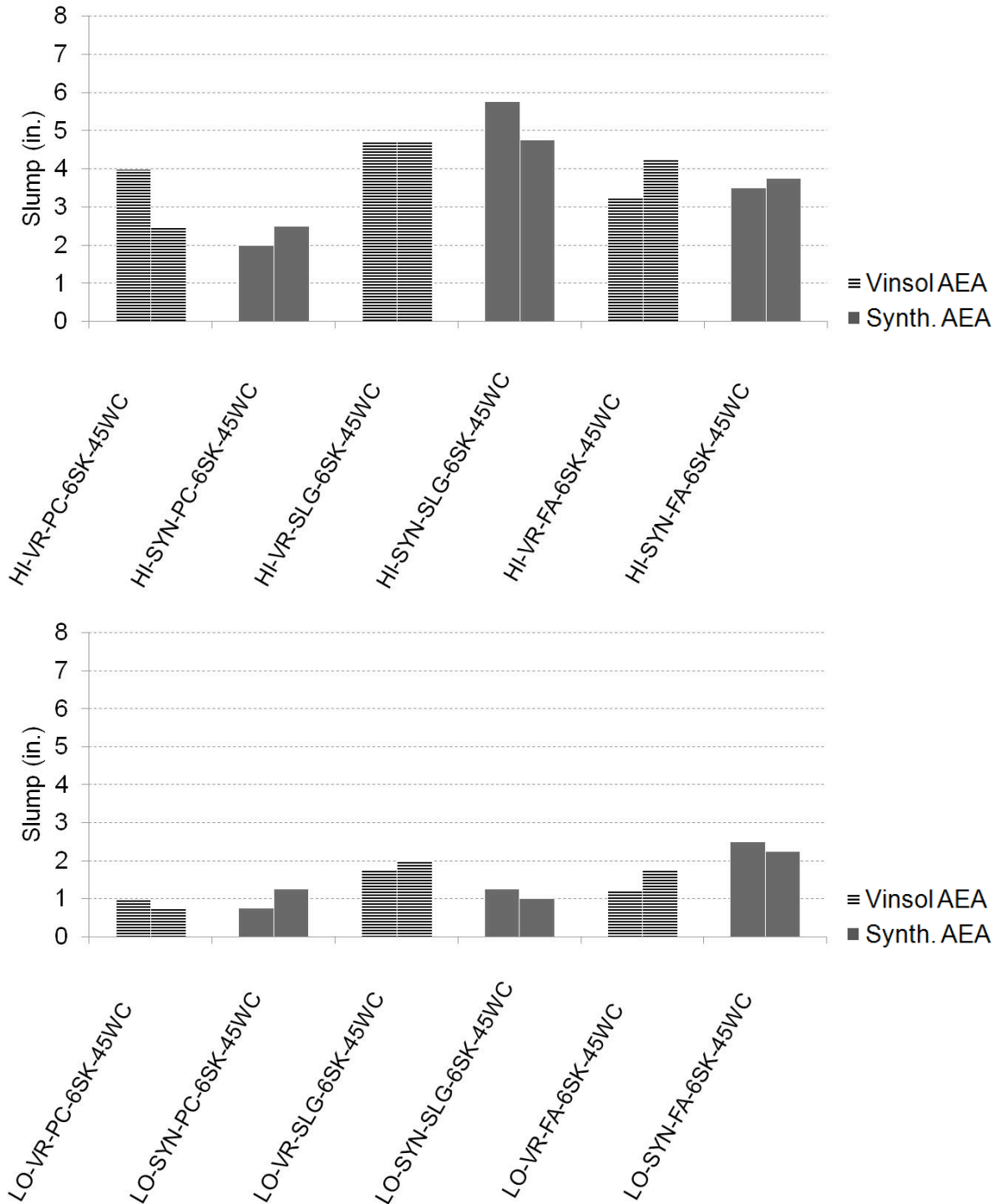


Figure 8: Slump of fresh concrete for Phase II 0.45 w/cm 564 lbs/yd³ CMC mixtures. From top to bottom, high air content and low air content mixtures. From left to right, straight portland cement mixtures, 40 wt. % substitution slag cement mixtures, and 25 wt. % substitution fly ash mixtures. Striped bars denote mixtures with vinsol resin AEA; solid bars denote mixtures with synthetic AEA.

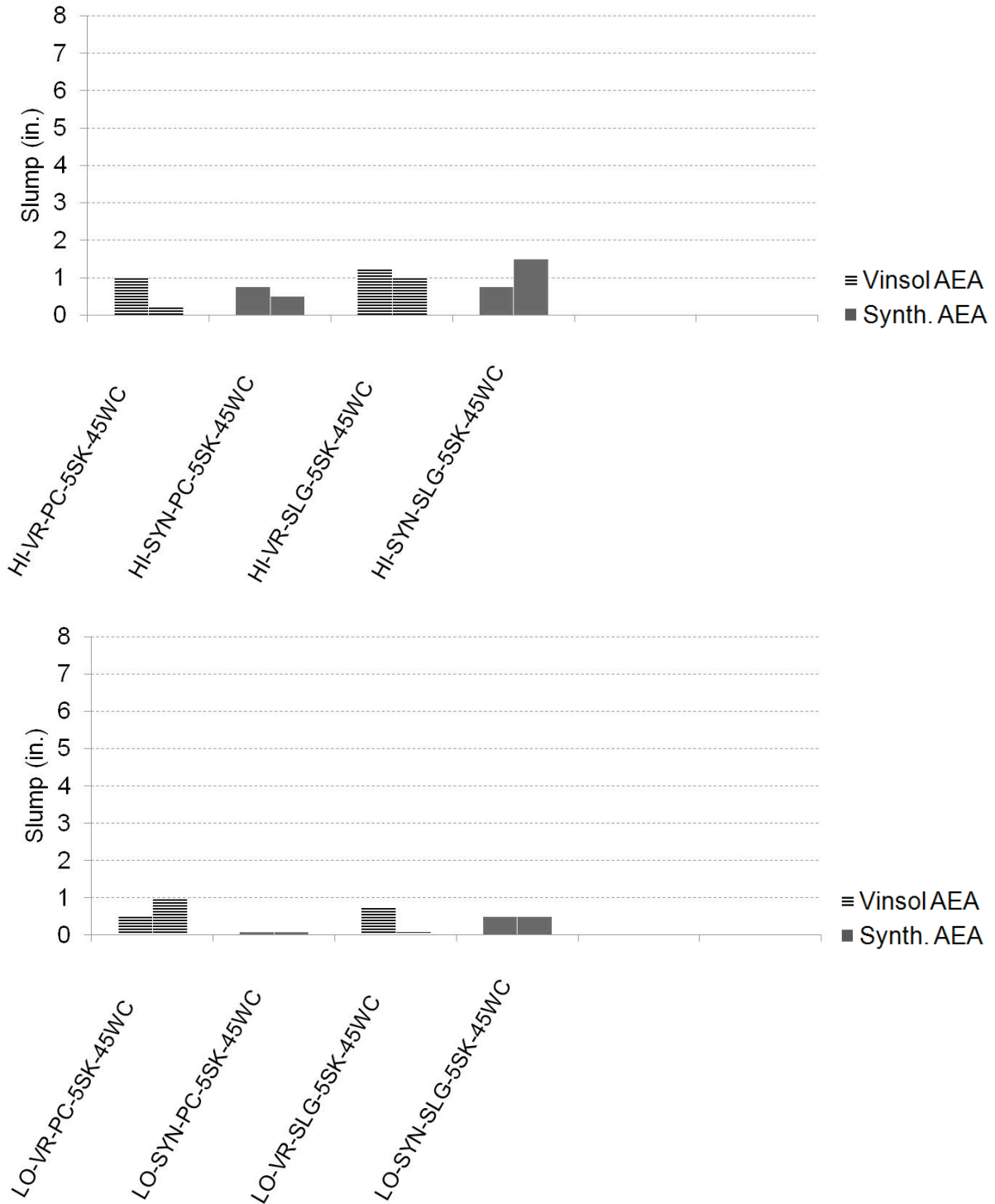


Figure 9: Slump of fresh concrete for Phase II 0.45 w/cm 470 lbs/yd³ CMC mixtures. From top to bottom, high air content and low air content mixtures. From left to right, straight portland cement mixtures and 40 wt. % substitution slag cement mixtures. Striped bars denote mixtures with vinsol resin AEA; solid bars denote mixtures with synthetic AEA.

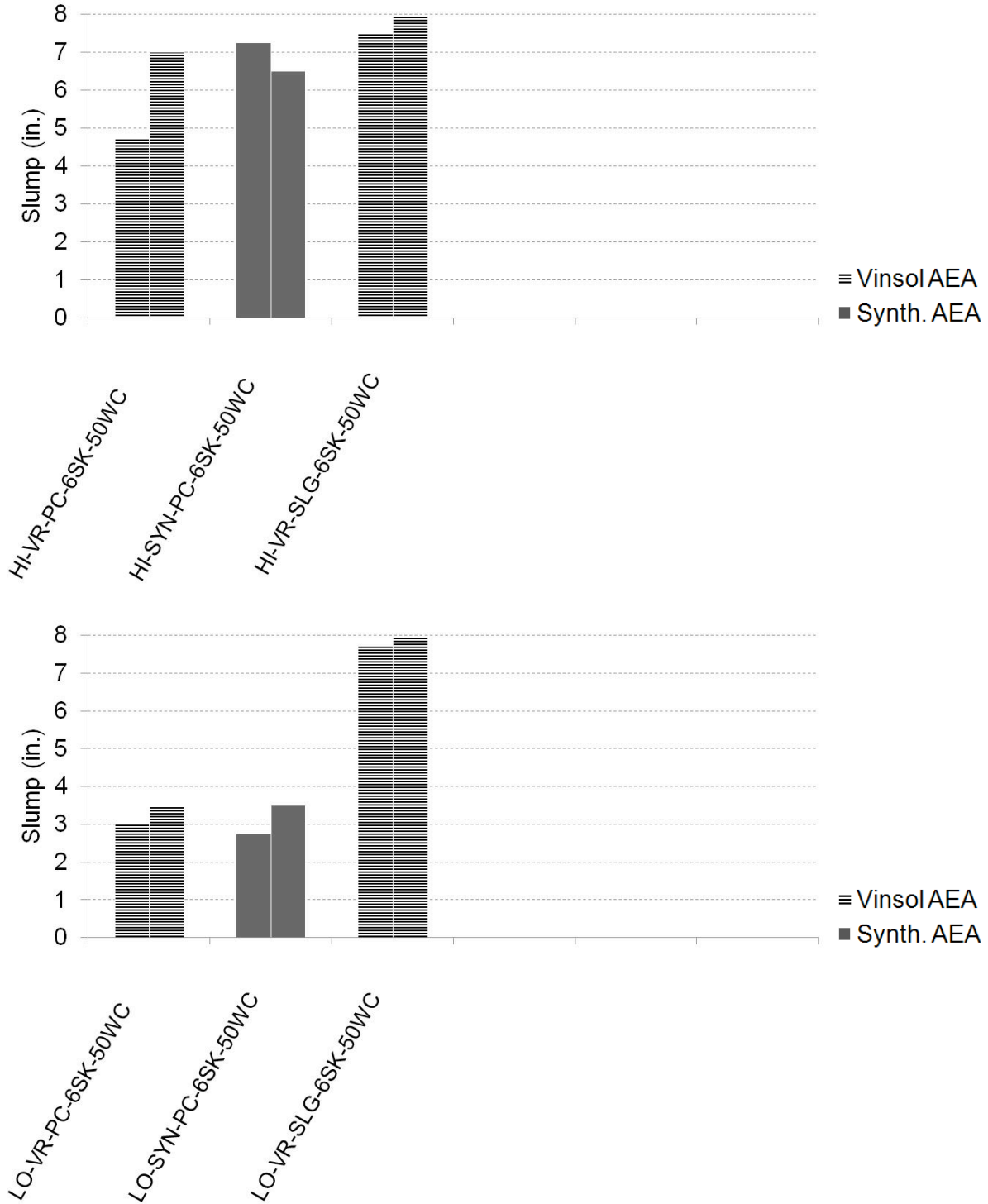


Figure 10: Slump of fresh concrete for Phase II 0.50 w/cm 564 lbs/yd³ CMC mixtures. From top to bottom, high air content and low air content mixtures. From left to right, straight portland cement mixtures and 40 wt. % substitution slag cement mixtures. Striped bars denote mixtures with vinsol resin AEA; solid bars denote mixtures with synthetic AEA.

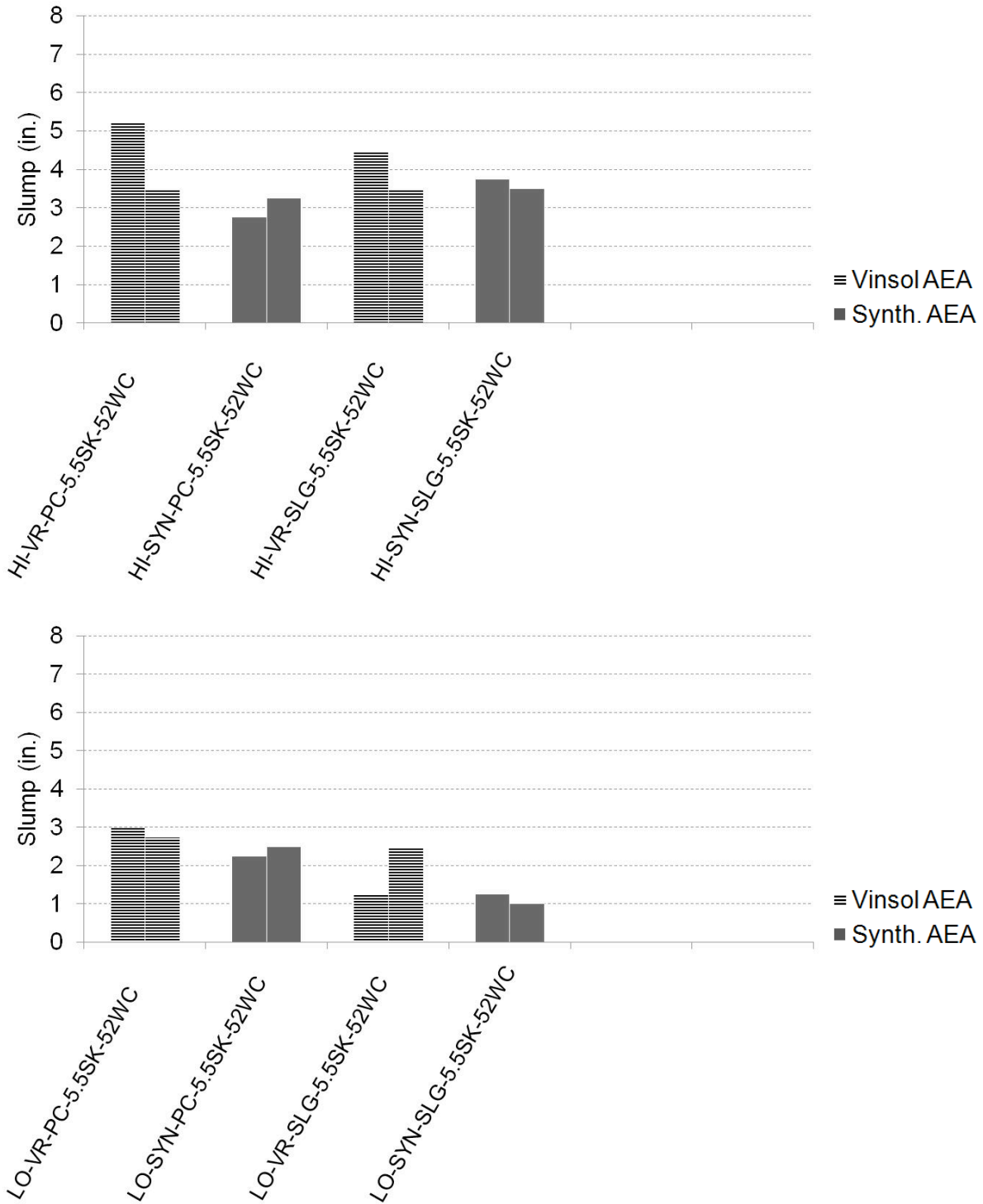


Figure 11: Slump of fresh concrete for Phase II 0.52 w/cm 517 lbs/yd³ CMC mixtures. From top to bottom, high air content and low air content mixtures. From left to right, straight portland cement mixtures and 40 wt. % substitution slag cement mixtures. Striped bars denote mixtures with vinsol resin AEA; solid bars denote mixtures with synthetic AEA.

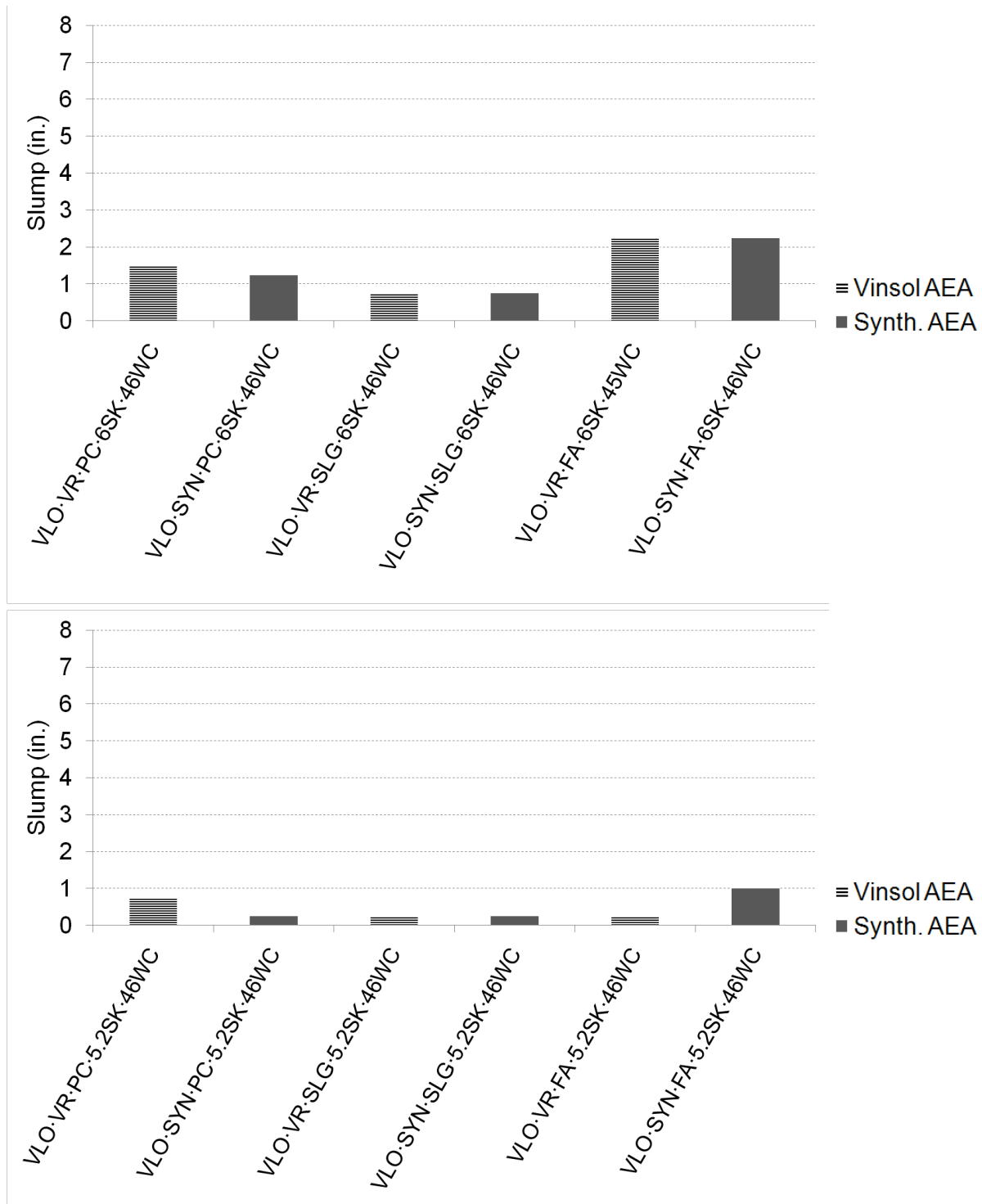


Figure 12: Slump of fresh concrete for Phase III 0.46 w/cm very low air content mixtures. From top to bottom, 564 lbs/yd³ and 490 lbs/yd³ CMC mixtures. From left to right, straight portland cement mixtures, 40 wt. % substitution slag cement mixtures, and 25 wt. % substitution fly ash mixtures. Striped bars denote mixtures with vinsol resin AEA; solid bars denote mixtures with synthetic AEA.

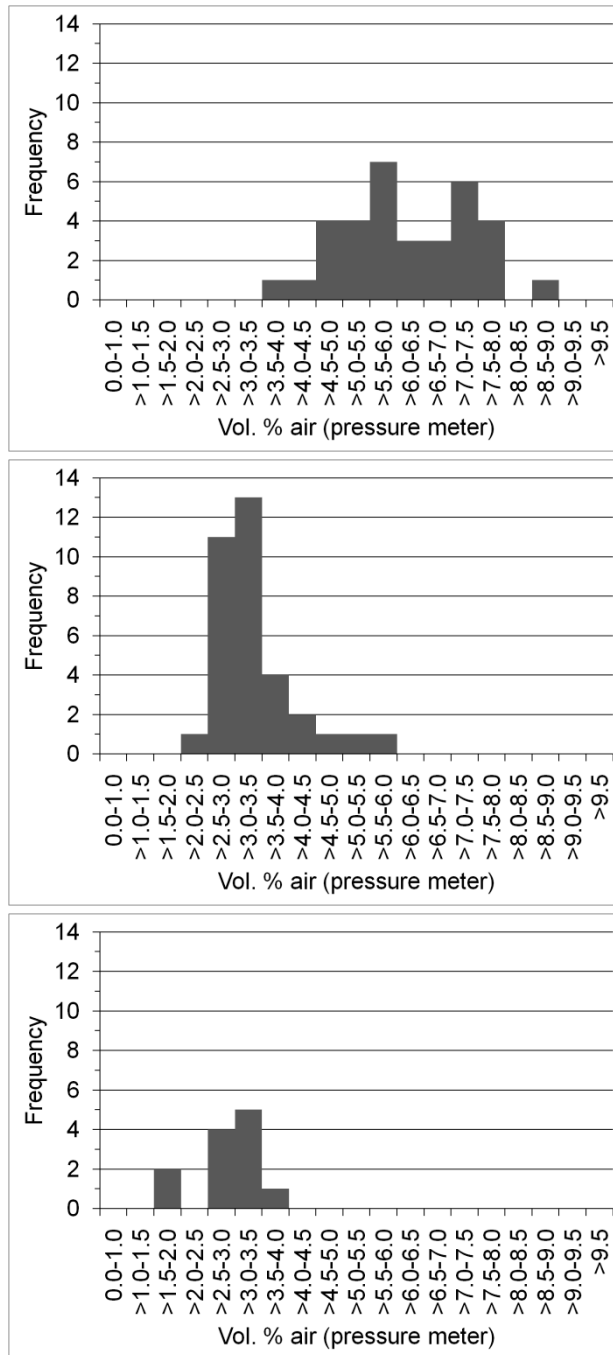


Figure 13: Air content pressure meter test results grouped according to mixture design target air contents. From top to bottom: Phase II high air content mixtures, (6.5 vol. % target) Phase II low air content mixtures, (3 vol. % target) and Phase III very low air content mixtures, (2 vol. % target).

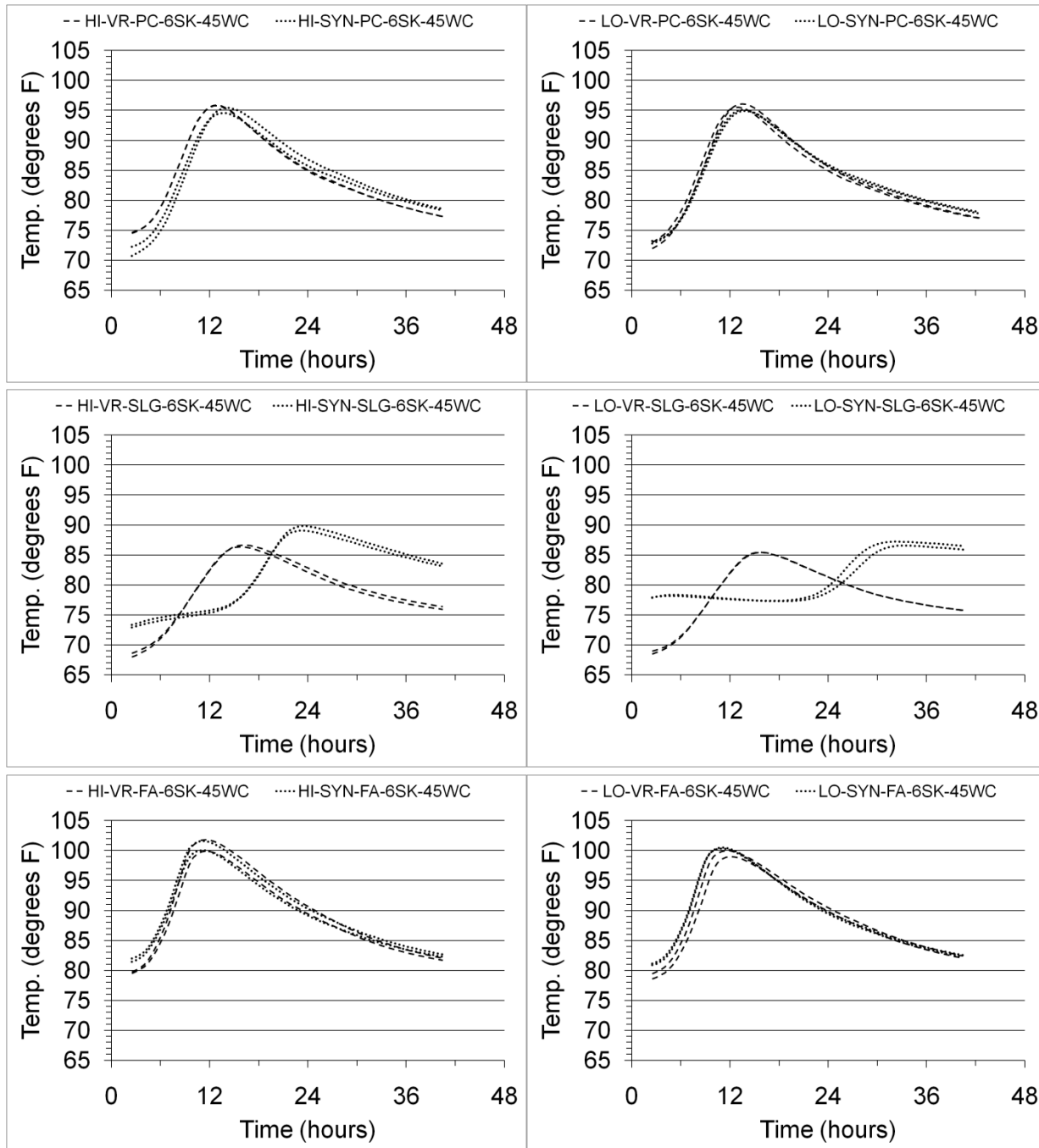


Figure 14: Calorimetry plots for the Phase II 0.45 w/cm^3 564 lbs/yd³ CMC mixtures. From left to right, high air content mixtures vs. low air content mixtures. From top to bottom: straight portland cement mixtures, 40 wt. % substitution slag cement mixtures, and 25 wt. % substitution fly ash mixtures. Dashed lines denote mixtures with vinsol resin AEA; dotted lines denote mixtures with synthetic AEA.

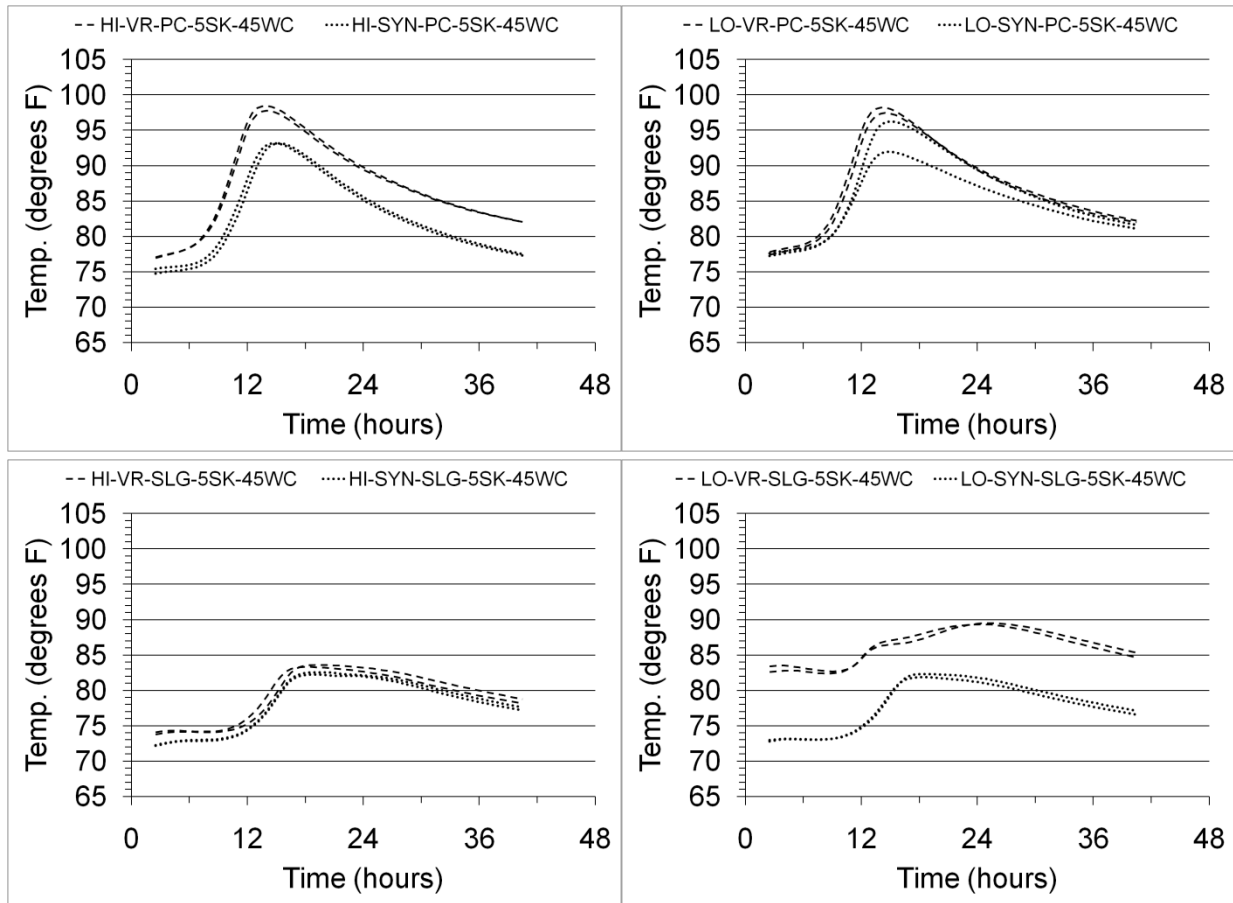


Figure 15: Calorimetry plots for the Phase II 0.45 w/cm 470 lbs/yd³ CMC mixtures. From left to right, high air content mixtures vs. low air content mixtures. From top to bottom: straight portland cement mixtures, and 40 wt. % substitution slag cement mixtures. Dashed lines denote mixtures with vinsol resin AEA; dotted lines denote mixtures with synthetic AEA.

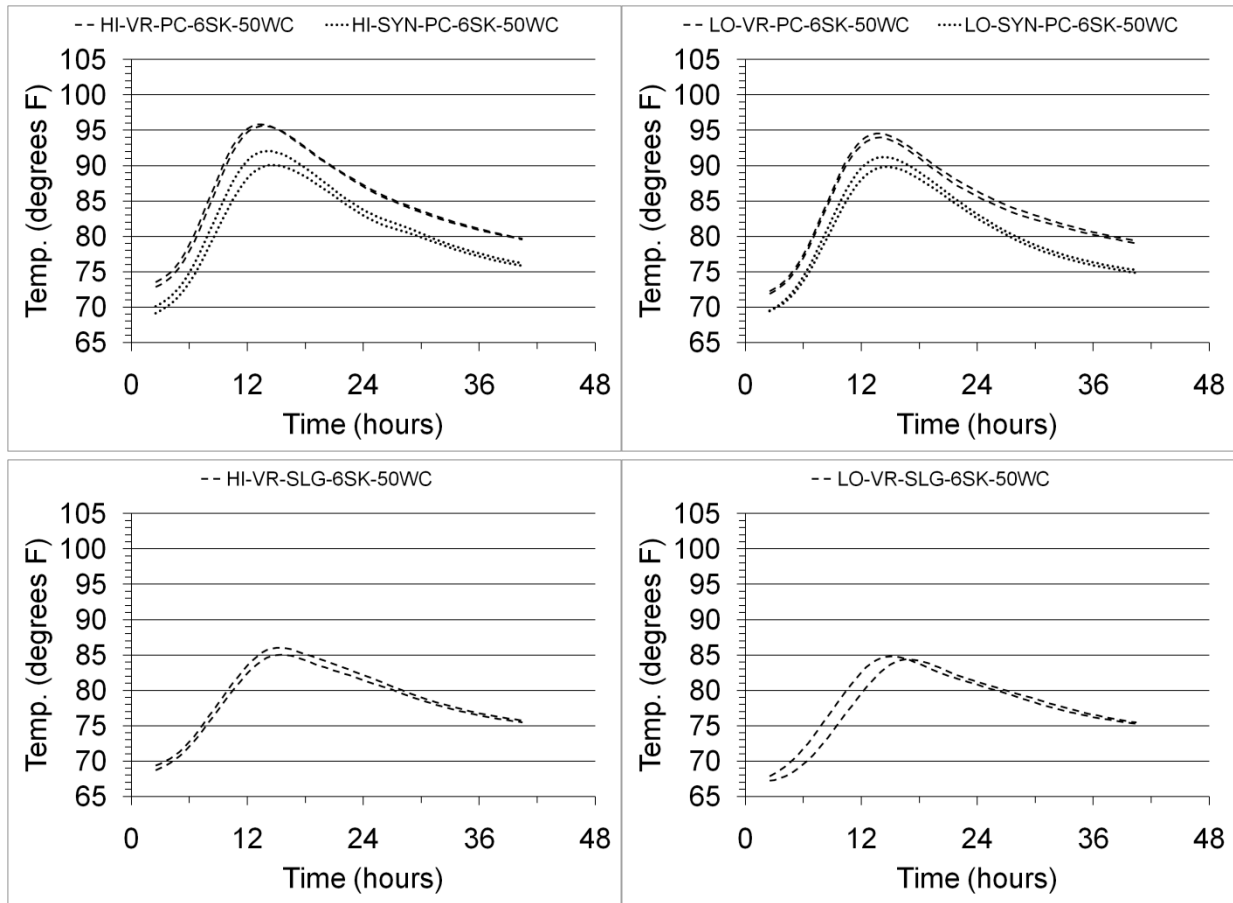


Figure 16: Calorimetry plots for the Phase II 0.50 w/cm 564 lbs/yd³ CMC mixtures. From left to right, high air content mixtures vs. low air content mixtures. From top to bottom: straight portland cement mixtures, and 40 wt. % substitution slag cement mixtures. Dashed lines denote mixtures with vinsol resin AEA; dotted lines denote mixtures with synthetic AEA.

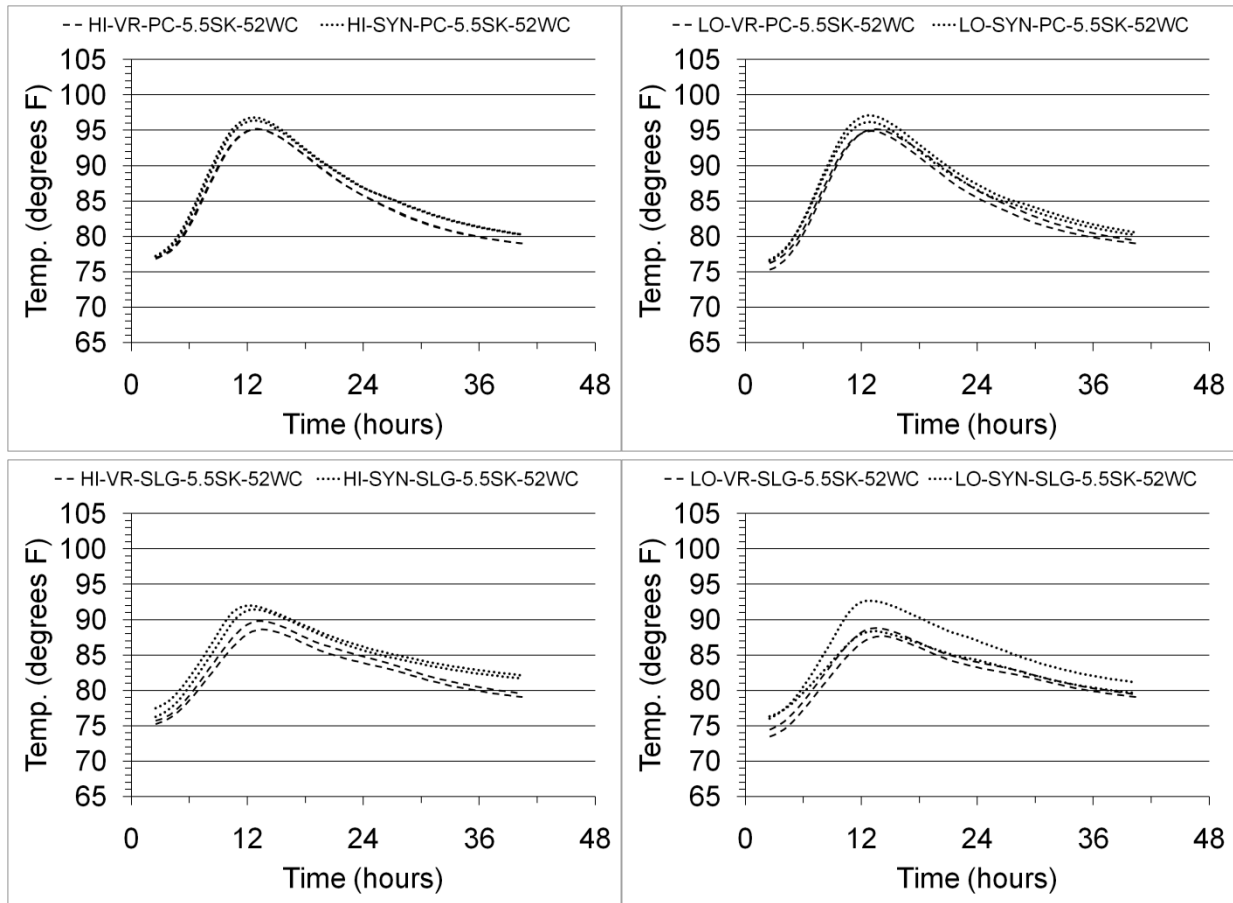


Figure 17: Calorimetry plots for the Phase II 0.52 w/cm 517 lbs/yd³ CMC mixtures. From left to right, high air content mixtures vs. low air content mixtures. From top to bottom: straight portland cement mixtures, and 40 wt. % substitution slag cement mixtures. Dashed lines denote mixtures with vinsol resin AEA; dotted lines denote mixtures with synthetic AEA.

5.1.3 Calorimetry Curves from Exploration of Delayed Set Mixture

Calorimetry is used to monitor the progress of cement hydration in a concrete mixture. Generally speaking, heat evolution as a result of cement hydration begins with an initial rapid spike and then subsequent rapid decrease in concrete temperature at the time of mixing (duration ~ 15 minutes), a dormancy period where the concrete is plastic and remains slightly above ambient temperature (duration ~ 2-4 hours), and then a hardening period where a steady increase in concrete temperature is observed as the concrete stiffens, commencing with the initial set and finalizing at final set (duration ~ 2-4 hours). These are followed by periods of cooling and then further densification through hydration. For the calorimetry plots shown in this report, the initial spike at mixing is not recorded.

As shown in Figure 14, the LO-SYN-SLG-6SK-45WC mixture experienced an approximate 24-hour delay in both initial and final set. The mixture was repeated at a later date, but at a lower laboratory ambient temperature, (74°F versus 78°F) and the previously observed delay of set did not occur. When the room temperature was higher, (81°F) two additional mixtures were repeated, one at room temperature, and another where the aggregates were heated prior to mixing, (86°F). Again, a delay in set did not occur for either elevated temperature mixtures. Figure 18 shows the calorimetry curves for the original delayed set mixture, and the subsequent attempts at repeating the delayed set phenomenon. The delay in set was suspected to be due to a complex interaction between the admixtures, temperature, and the chemical composition of the slag and the portland cement. Two additional elevated temperature mixtures were repeated, one at room temperature (84°F) and one with heated aggregates (92°F) but with double the dosage of water reducer as in the original delayed set mixture. Again, a delay in set did not occur in either increased dosage water reducer mixtures. Figure 19 shows the calorimetry curves for the original delayed set mixture and the increased dosage water reducer mixtures.

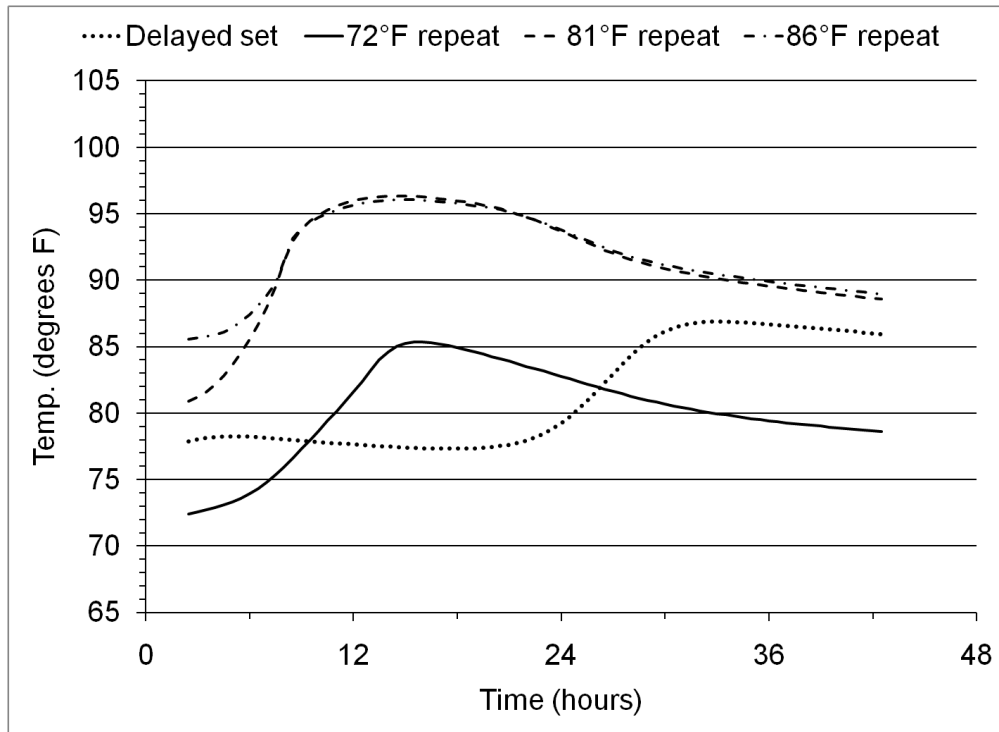


Figure 18: Calorimetry curves for delayed initial and final set mixture and repeat mixtures.

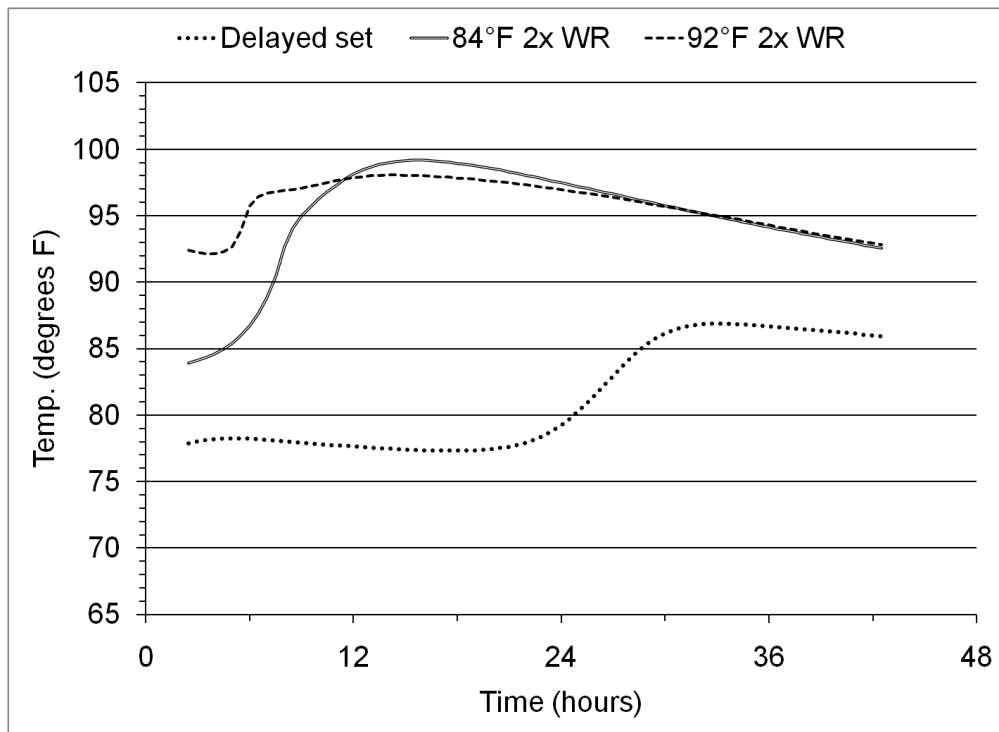


Figure 19: Calorimetry curves for delayed set mixture and repeat mixtures with double the water reducer dosage.